Elucidating the Function of Krüppel Homolog 1 (Kr-h1) Associated Proteins (KAPs) in *Aedes aegypti* Reproduction Through RNA Interference-Mediated Downregulation

Liyan Zhang

Thesis submitted to the Faculty of the Virginia polytechnic Institute and State University in partial fulfillment of the requirements for the degree of

Master of Science in Life Science in Biochemistry

Jinsong Zhu, Chair

Zhijian Tu

Chloé A Lahondère

June 13, 2024

Blacksburg, Virginia

Keywords: Mosquito, *Aedes aegypti*, Krüppel homolog 1 (Kr-h1), dimerization partner (DP-1), RNA interference (RNAi), Co-immunoprecipitation (Co-IP), embryogenesis

Elucidating the Function of Krüppel Homolog 1 (Kr-h1) Associated Proteins (KAPs) in *Aedes aegypti* Reproduction Through RNA Interference-Mediated Downregulation

Liyan Zhang

Abstract (Academic)

The transcription factor Krüppel homolog 1 (Kr-h1) is crucial in multiple reproductive processes of *Aedes aegypti* mosquitoes, including previtellogenesis, vitellogenesis, and oogenesis. This study explores the interaction between Kr-h1 and its potential associated proteins (KAPs), with a specific focus on the dimerization partner (DP-1), and how this interaction regulates gene expression pathways critical for mosquito reproduction. Utilizing RNA interference (RNAi), the research identifies DP-1 as a significant regulator of follicle growth post-eclosion (PE), highlighting its vital role in the mosquito reproductive regulatory pathway. The experimental approach included RNAi-mediated knockdown of DP-1, accompanied by evaluations using quantitative PCR (qPCR), Western blotting (WB), co-immunoprecipitation (Co-IP), follicle length measurement, and egg counting to assess the role of DP-1 in reproductive functions. For the first time, the inhibition of DP-1 expression was found to significantly impede *A. aegypti* follicular development. The elucidation of the mechanistic roles of Kr-h1 and DP-1 provides valuable insights that could lead to innovative strategies for mosquito population control and effective disease vector management.

Elucidating the Function of Krüppel Homolog 1 (Kr-h1) Associated Proteins (KAPs) in *Aedes aegypti* Reproduction Through RNA Interference-Mediated Downregulation

Liyan Zhang

Abstract (General audience)

Mosquitoes can spread serious insect-borne diseases such as dengue, Zika, and malaria, etc. These diseases can infect hundreds of millions of individual and cause around a million of death annually. This study focuses on a specific mosquito species, *Aedes aegypti*, which is a major carrier of these diseases. To manage their populations and reduce the spread of these diseases, scientists are constantly seeking new methods to control their reproduction. Chemical insecticides are one of the most efficient and widely used strategies. However, these insecticides face significant challenges, including the development of resistance in mosquito populations and the potential damage to non-target species to affect the ecosystem. To address this issue, the development of new insecticides is crucial. We can identify new targets to pave the way to research novel effective insecticides. Inside mosquitoes, there are various proteins that help control their ability to reproduce. One of these proteins is called Krüppel homolog 1 (Kr-h1). Kr-h1 plays a crucial role in the development and reproductive processes of mosquitoes. Our research looked at how Kr-h1 interacts with other types of protein to control mosquito reproduction. Through various experiments, including gene expression analysis and protein studies, we found that DP-1 is essential for the proper development of mosquito eggs. This insight helps us understand more about the biological processes and hormonal pathways during mosquito reproduction, therefore provide greater opportunity to develop insecticides to reduce their populations and the spread of the diseases they carry.

Acknowledgement

I would like to express my gratitude to the Department of Biochemistry at Virginia Tech for enriching my graduate experience. The department has significantly enhanced my academic and research skills, as well as my abilities in collaboration and communication. This comprehensive development has prepared me to pursue my Ph.D. studies at IGEP program in the future.

I am deeply grateful to my Ph.D. advisor, Dr. Jinsong Zhu, for his invaluable guidance, unwavering support, and patience throughout my research. His direction has been instrumental in successfully shaping my projects and ensuring their steady progress. He has provided an ideal atmosphere for practicing independent and critical thinking, allowing me to navigate my research effectively. I especially appreciate his flexibility in accommodating my unconventional work hours, enabling me to work in the afternoons and nights. His understanding and support have made my challenging graduate life more manageable and less stressful.

I would also like to express my heartfelt gratitude to my committee members, Dr. Jake Tu and Dr. Chloé Lahondère, for their patience and inspiration. Their seminars and my rotation periods with them have been enlightening, helping me to better understand the current state of my research field. Their insights and encouragement have been invaluable in shaping my academic journey.

I also extend my sincere gratitude to all the past and present members of Dr. Zhu's lab— Maria Dorodnitsyna, Katara Griffith, Wenhao Zhao, and Randy Saunders—for their invaluable mental support and precious assistance, help with my projects and experiments, and guidance in my research have been instrumental to my success. Their guidance and encouragement greatly relieved my anxiety during my graduate life. I am truly grateful to meet them.

I feel fortunate to have lived in Blacksburg for the past six years. This peaceful town has become my 'second' home, fostering my patience and personal growth. During my time here, I have met many wonderful classmates and friends. Spending quality time with them, engaging in meaningful discussions, and participating in various activities during my spare time has greatly relieved my mental pressure.

Last but not least, I want to express my utmost love and gratitude to my father, mother, grandma, and aunts in China. They have always stood by my side through good times and bad, providing invaluable support. Without them, pursuing my M.S. would not have been possible. I also deeply appreciate my elder cousin in Washington D.C. for offering various forms of support over the past several years.

List of Abbreviations

20E	hydroxyecdysone
3-AT	3-Amino-1,2,4-triazole
AD	activation domain
bHLH	beta helix loop helix
Br-C	broad complex
CA	corpora allata
CaMKII	Calcium/Calmodulin-dependent protein kinase II
CFR	case fatality rate
CHIKV	chikungunya
DAG	diacylglycerol
DBD	DNA-binding domain
DP-1	dimerization partner-1
E93	Ecdysone-induced protein 93F
EcR	ecdysone receptor
ER	endoplasmic reticulum
FOXO	Forkhead box O
Gce	Germ cell-expressed
Hsp83	heat shock protein 83
IIS	Insulin/Insulin-like Growth Factor Signaling
ILP	Insulin-like peptide
IP3	inositol 1,4,5-trisphosphate
JH	juvenile hormone
JH-III	juvenile hormone III
JHRE	juvenile hormone response elements
KAPs	Kr-h1 associated proteins
Kr-h1	Krüppel Homolog 1
Met	methoprene tolerant
MVAP	mevalonic acid pathway
Nup	nucleoporin
OEH	ovarian ecdysteroidogenic hormone
PBM	post blood meal
PDGF	platelet-derived growth factor
PE	post-eclosion
PIP2	phosphatidylinositol 4,5-bisphosphate
PKC	protein kinase C
PLC	phospholipase C
PPF	pyriproxyfen
PVR	PDGF VEGF receptor
RTKs	receptor tyrosine kinases
RVF	rift Valley fever
Tai	Taiman

TOR	target of rapamycin
TF	transcription factor
TPR	tetratricopeptide repeat
UAS	upstream activating sequences
USP	Ultraspiracle
VEGF	vascular endothelial growth factor-related receptor
Vg	vitellogenin
VSSC	voltage-sensitive sodium channel
YFV	yellow fever
ZnF	zinc finger

List of insect species binomial nomenclature

A. aegypti	*Aedes aegypti*
A. mellifera	*Apis mellifera*
B. mori	*Bombyx mori*
C. septempunctata	*Coccinella septempunctata*
C. carnea	*Chrysoperla carnea*
D. melanogaster	*Drosophila melanogaster*
L. migratoria	*Locusta migratoria*

Table of Contents

Chapter 1: Introduction and Significance

1.1 Mosquito-transmitted Diseases and Current Control Measures

Mosquitoes rank as the world's most lethal animals; over 1 million people die due to the spread of vector-borne diseases each year globally (**Fig 1**). Within thousands of species of mosquitoes, the hematophagous *Aedes* vector plays a pivotal role in spreading deadly flaviviruses including but not limited to Zika, dengue, chikungunya (CHIKV), yellow fever (YFV), and Rift Valley fever (RVF)[1] (**Table 1**). These diseases significantly contribute to the global burden of infectious diseases and a considerable amount of research has been devoted to inhibiting their spread.

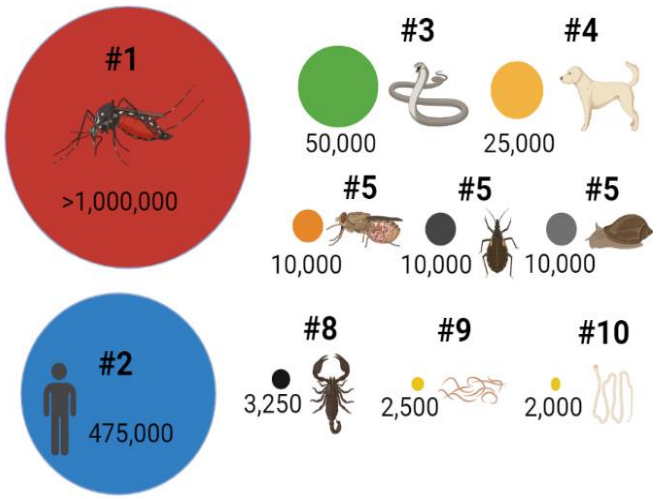

Figure 1. *Comparative Annual Human Mortality by Animal. Mosquitoes, depicted at #1, are the leading cause of animal-related human deaths, exceeding 1 million per year, significantly more than human-induced fatalities and other animals. The Data source comes from https://www.cnet.com/pictures/the-24-deadliest-animals-on-earth-ranked/23/*

Zika virus has seen outbreaks in over 85 countries despite the suitability of 215 countries (86% of countries on earth) for the *Aedes* species[1]. This virus has garnered significant attention due to its association with severe neurological complications, microcephaly, and congenital anomalies, especially in fetuses and infants that spread from their mothers vertically[2-3]. Dengue fever stands out as the most pervasive of these diseases transmitted horizontally, reported in 111 countries, highlighting an escalating public health challenge. About half of the global population can be threatened by Dengue virus, and up to 400 million infection cases annually, mainly distributed in urban and suburban areas[14].

CHIKV and YFV have also shown significant spread, with CHIKV reported in 106 countries and YFV in 43 countries, determining the potential risk these viruses pose[1]. CHIKV would induce intense fever and joint discomfort, with around 40% of infected individuals experiencing prolonged rheumatic issues that can last from several months to years, and there are no specific drugs on commercial vaccine that can be applied to treat CHIKV[4]. YFV could cause up to 180,000 fatal cases in Africa despite its presenting symptoms like other arboviruses, such as vomiting, muscle aches, and fever. YFV distinguishes itself with its potential for a high in-hospital case fatality rate (CFR), which can reach up to 67% [5]. RVF, though

primarily reported in the Middle East and Africa, also represents an emerging zoonotic threat with the potential for inconsistent wider spread and lack of specific medicines or commercial vaccines, given the

Table 1*. Count of countries/territories conducive to vector habitation and count of countries/territories impacted by the diseases, categorized by region.*

	Countries/territories affected by vector & mosquito-borne diseases					
Global Region	***Aedes aegypti***	Yellow Fever (YFV)	Dengue Fever	Zika Virus	Rift Valley Fever (RVF)	Chikungunya (CHIKV) Fever
Africa	**56**	30	36	14	36	26
Americas	**52**	13	46	48	0	46
Oceania	**23**	0	11	12	0	11
Asia	**45**	0	15	11	3	20
Europe	**12**	0	3	0	0	3
Overall	**188**	**43**	**111**	**85**	**39**	**106**

global distribution of its vector[6]. In addition, these diseases have many common symptoms, such as fever and muscle ache, which can be easily misdiagnosed, especially in regions that don't have advanced medical conditions and hygiene environments. The lack of target drugs or vaccines further increases the burden of medical resources (**Table 2**).

Among thousands of mosquito species, *Aedes aegypti*, one of the dominant vectors that spread deadly arboviral diseases, consistently induces substantial public health challenges across tropical, subtropical, and even some temperate regions worldwide[10-11]. *A. aegypti* are most active during dawn and dusk, and they can bite various targets multiple times[14]. After the arbovirus replicates within the *A. aegypti* through its primary feeding behavior, typically within its midgut, the virus migrates to the salivary glands and the virus can be transmitted to a new human host through the mosquito's saliva during subsequent blood meals[7]. The global proliferation of *A. aegypti*, aggravated by human activities such as international shipping and trade, along with recent decades of climate change, has significantly broadened the distribution of vector-

borne diseases, reinforcing the ability of *A. aegypti* as a critical vector in the transmission cycle[8]. Understanding the physiological and reproductive behaviors of *A. aegypti* is essential to unravel the spread dynamics of these diseases and critical for the formulation of effective vector control strategies[12].

Aede's global spread, coupled with its exceptional efficiency as a vector, is largely due to its co-evolutionary history with arboviruses and humans in Africa, which has optimized its ability to transmit these diseases[7]. Its dominance as a vector outside Africa proves its capacity to adapt to various environments and its close association with human habitats, making it a formidable vector to transmit current and potentially future viral pandemics[7]. Focusing on *A. aegypti* offers a strategic advantage in simultaneously relieving the spread of multiple mosquito-borne diseases, presenting a more efficient and cost-effective approach to reducing disease burden and preventing future outbreaks.

Table 2. WHO Approved Vaccines and Drugs for Arbovirus-Related Diseases. *Vaccines are only available for YFV and Dengue Fever. No vaccines or drugs are approved for Zika, RVF, or CHIKV.*

Arbovirus	YFV	Dengue Fever	Zika	RVF	CHIKV
Vaccine	17D live-attenuated	Dengvaxia (CYD-TDV)	none	none	none
Drug	none	none	none	none	none

The cornerstone of combating mosquito-borne diseases has long relied on the neurotoxic effects of pyrethroids due to their widespread effectiveness in controlling adult mosquito populations[29]. Pyrethroid can disturb the function of the voltage-sensitive sodium channel (VSSC) in insect nerve cells and delay the channel closure during neural signal transmission, causing prolonged nerve excitation and eventually paralysis and killing the vectors[9]. However, despite its low toxicity to mammalian and minimal environmental effects, the extensive emergence of resistance to pyrethroids within wide mosquito populations is undermining these efforts, resulting in a critical challenge to vector management strategies[17]. This resistance, marked by P450-monooxygenases detoxification that metabolizes xenobiotics such as insecticides and mutations in the VSSC that decrease the sensitivity of VSSC to pyrethroids, varies geographically but is highly prevalent in *Aedes* species[18]. This emphasizes the urgency for innovative control measures that circumvent existing resistance mechanisms.

1.2 Mosquito Life History and Reproduction

An effective vector control strategy begins with an intricate understanding of the *A. aegypti* lifecycle, which comprises four distinct stages: eggs, larvae, pupae, and adults. Eggs are laid individually in a variety of natural and artificial water-holding containers, including but not limited to bird baths, flowerpots, discarded tires, clogged gutters, etc. Their eggs can withstand desiccation for several months to half a year without sustaining damage. This resilience allows for survival through fluctuating surviving conditions, including both endophilic (indoor) and exophilic (outdoor) environments[28]. The emergent larvae undergo four developmental instars over the course of approximately 5-6 days, thriving in an aquatic habitat. The fourth-instar larval stage is marked by wandering behavior in preparation for pupation. Following the non-feeding pre-pupal stage transition, metamorphosis is activated, culminating in adult mosquitoes' emergence within two days. Adult size is fixed post-emergence, with mating usually ensuing rapidly.

Adult *Aedes* intake plant-derived sugar, such as glucose, to support physiological activity, and females specifically require a blood meal to facilitate embryogenesis, marking the onset of their reproductive cycle[21].The reproductive cycle and behavior of *A. aegypti* are intimately correlated to the dynamics of disease spread. Females seek blood meals primarily during dawn and dusk, coinciding with their peak activity periods. The ingested blood provides the necessary nutrients to produce certain transcription factors (TF) to activate egg maturation-related signal transduction pathways [21]. A pivotal yolk protein, vitellin, is essential for mosquito egg development and is synthesized from its precursor, vitellogenin (Vg)[46]. This process, known as vitellogenesis, produces Vg from the fat body and releases it into the hemolymph[19]. It eventually crosses the follicular epithelium and is taken up by the Vg receptors on the developing oocytes in the ovaries to process into vitellin. This mechanism is orchestrated by the acyclic sesquiterpenoid juvenile hormone (JH) and molting hormone 20-hydroxyecdysone (20E), which regulate the production of Vg in response to specific carbohydrates and proteins derived from the ingested blood. Targeting these vitellogenesis-related hormonal pathways can potentially disrupt egg

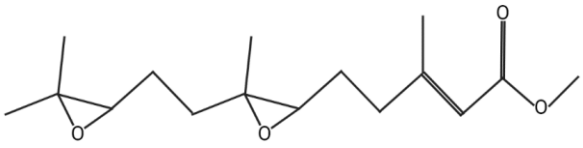

***Figure 2**. The chemical structure of acyclic sesquiterpenoid Juvenile hormone (JH)*

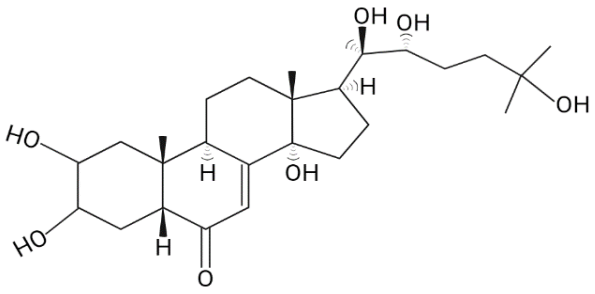

***Figure 3**. The chemical structure of steroid hormone 20-hydroxyecdysone (20E)*

maturation, significantly curtailing mosquito embryogenesis, oviposition, egg hatching, and, consequently, the transmission of vector-borne diseases. Understanding the hormonal regulation in *A. aegypti* reproduction, specifically the roles and interplay of JH and 20E, is fundamental to comprehend the lifecycle of mosquito. This knowledge presents a potential target for novel interventions aimed at mosquito population management and disease control. By disrupting the hormonal pathways that regulate vitellogenesis and other reproductive processes, we can develop strategies that reduce the reproductive success of *A. aegypti*, thereby lowering the population and the incidence of mosquito-borne diseases.

1.3 JH Regulation of Mosquito Reproduction

Juvenile hormone (JH) is highly conserved across insect taxa and serves as a pivotal regulator orchestrating their life pattern. It plays important roles during metamorphosis and adult reproduction. Utilizing low doses of JH analogs like pyriproxyfen (PPF) in larvicidal applications highlights the effectiveness of targeting this hormone pathway in mosquito[31-33]. PPF is associated with the Methoprene-tolerant (Met) and acts as an agonist ligand to regulate insect growth[34]. Exposure to pyriproxyfen (PPF), significantly impairs both embryogenesis and morphogenesis in adult mosquitoes. However, given that JH signaling is highly conserved among other insects, such as *Apis mellifera, Coccinella septempunctata, Chrysoperla carnea*, etc. The overuse of JH mimics could disrupt the stability of local ecosystems to result in worse side effects. This concern emphasizes the importance of understanding JH signaling pathways, which consist of a cascade of transcriptional regulators controlling gene expression responses to JH. These pathways intricately interact with those genes governed by 20-hydroxyecdysone (20E), the hormone that promotes metamorphosis in

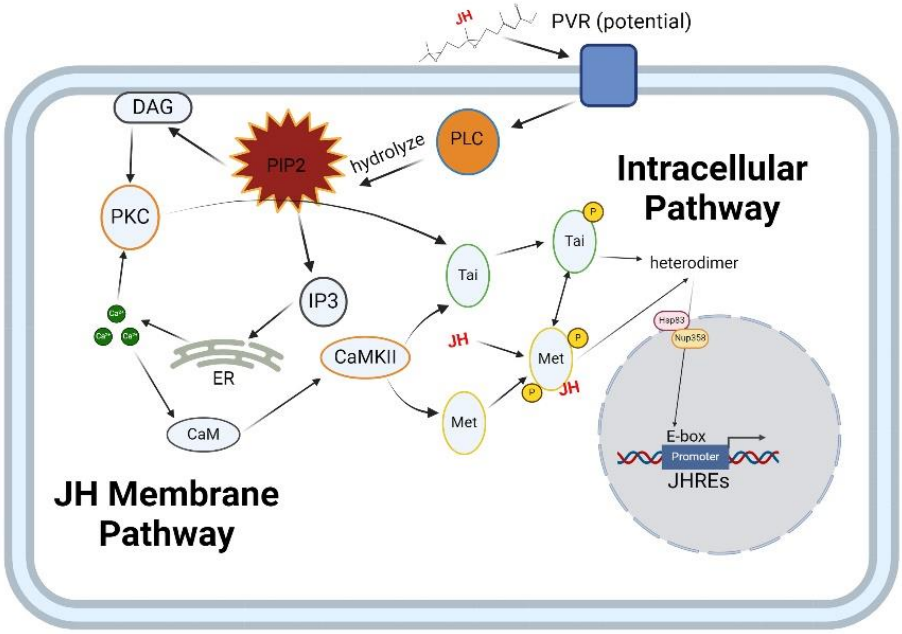

Figure 4. Juvenile Hormonal (JH) regulation pathways in Aedes aegypti. *The diagram illustrates the dual action of juvenile hormone (JH) via the intracellular Met/Taiman complex and a membrane-associated pathway involving the receptor tyrosine kinases (RTKs) - PDGF/VEGF-related receptor (PVR) and downstream signaling molecules to affect Kr-h1 gene expression.*

both hemimetabolous and holometabolous insects. While 20E drives the metamorphic processes, JH mitigates these effects, ensuring that larvae reach the appropriate size for molting without undergoing premature metamorphosis, thereby sustaining normal growth and development.

Juvenile Hormone III (JH-III), the predominant form of JH in dipteran insects such as *Drosophila melanogaster* and *A. aeypti*, plays a pivotal role in reproductive mechanisms. Unlike JH-I and JH-II, JH-III has fewer methyl groups and a shorter carbon side chain, contributing to its specific biological functions[115, 116] (**Fig 2**). JH-III is synthesized in the corpora allata (CA), the endocrine glands located on the posterior side of the brain, via the mevalonic acid pathway (MVAP). Following its synthesis, JH-III is directly secreted into the hemolymph, where it stimulates vitellogenin (Vg) production through the insulin-like peptide (ILP) pathway[21, 24].

In the previtellogenic stage of female beetles, JH treatment upregulates ILP, which in turn induces the phosphorylation of Forkhead box O (FOXO) via the ILP signaling pathway[47]. Initially, FOXO is localized to the FOXO response elements in the Vg promoter within the nucleus, where it inhibits Vg expression. However, upon phosphorylation by the ILP pathway, FOXO detaches from the Vg promoter, thereby permitting its activation by the JH pathway. This intricate signaling cascade underscores the regulatory role of JH-III in coordinating reproductive processes. Although this signal transduction pathway has been well-characterized in beetles, whether it is conserved in *A. aegypti* remains to be confirmed.

1.4 Molecular Action of JH and 20E

JH pathway: In the intracellular JH signaling cascade of *A. aegypti*, same as its analog PPF, JH binds to its cytoplasmic receptor Met to induce its conformational change that capable pairs with a p160 steroid receptor coactivator and obligatory DNA binding partner Taiman (Tai), which was also specifically called FISC in *A. aegypti,* to form a heterodimer[45]. The nuclear entry of this complex is mediated by the chaperone protein heat shock protein (Hsp83), which binds to Met's bHLH and PAS-B domains to stabilize it. The association between Hsp83 and nucleoporin (Nup358), particularly Nup358's tetratricopeptide repeat (TPR) domain, is critical for shuttling Met into the nucleus via the nuclear pore[24]. Inside the nucleus, the Met-Tai heterodimer binds to the E-box sequence CACGTG or E-box like sequence CACGCG in juvenile hormone response elements (JHREs) from the promoter of Kr-h1, initiating its transcription[21].

JH also triggers a less defined, alternative signaling pathway at the cell membrane, potentially involving receptor tyrosine kinases (RTKs) (**Fig 4**). Unpublished results in Dr. Zhu's lab have shown that PDGF (Platelet-Derived Growth Factor)/VEGF (Vascular Endothelial Growth Factor)-related receptor (PVR)

plays a key role in this process. Activation of RTKs could catalyze a cascade involving phospholipase C (PLC), which hydrolyzes phosphatidylinositol 4,5-bisphosphate (PIP2) into inositol 1,4,5-trisphosphate (IP3) and diacylglycerol (DAG). The second messenger IP3 facilitate the release of calcium ions from the endoplasmic reticulum (ER), activate Calcium/Calmodulin-dependent protein kinase II (CaMKII) and protein kinase C (PKC). The activated CaMKII can phosphorylate the Tai and Met to promote the intracellular signal transduction pathway to urge the expression of transducer Kr-h1[23]. These convergent pathways indicate the intricate regulatory architecture underpinning Kr-h1's role in insect development and physiology background Information.

20E pathway: 20E is characterized by a core steroid framework with four fused rings and hydroxyl groups attached at specific positions (**Fig 3**). Upon binding to steroid hormone 20E, the ecdysone receptor (EcR) forms a heterodimer with PKC phosphorylated Ultraspiracle (USP) and often recruits Tai as a transcriptional coactivator to form a functional unit capable of recognizing ecdysone response elements within the genome[24]. This hormone-receptor interaction activates ecdysteriodogenesis, a transcriptional cascade that regulates genes responsible for insect molting and metamorphosis (**Fig 5**). Key downstream TFs regulated by 20E signaling include Ecdysone-induced protein 93F (E93), critical for metamorphosis, and Broad-Complex (Br-C), integral for pupal development[24] (**Fig. 6**). In the cell line from *Bombyx mori*, Kr-h1 has been confirmed capable of binding to the Kr-h1 binding site (KBS) to the promoter region of Br-C and E93, which explains the rationality of JHM to downregulate the 20E pathway[44].

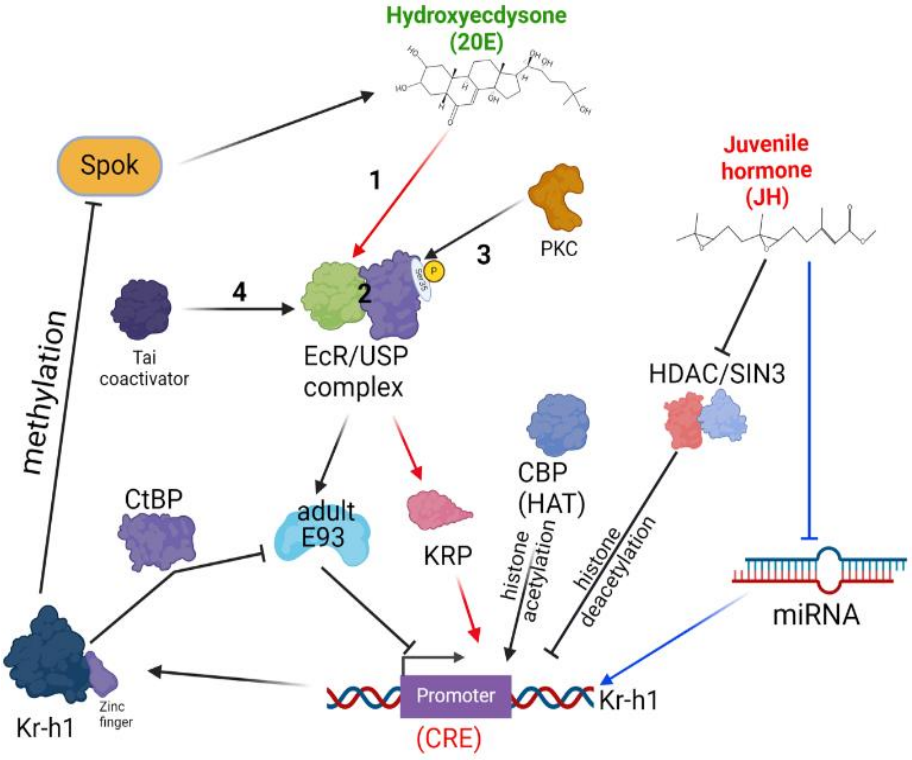

Figure 5. The signal transduction and posttranslational modification between JH, 20E, and Kr-h1. *The membrane-associated pathway activated protein kinase C (PKC) integrates with the 20-hydroxyecdysone (20E) pathway through the phosphorylation of USP Ser35 on the EcR/USP complex, therefore regulates the 20E-response genes that are related to metamorphosis, vitellogenesis, and embryogenesis in the mosquito life cycle.*

In dipterans such as *Drosophila melanogaster* and *A. aegypti*, the Vg expression is partially induced by 20E and ecdysone signaling pathway. The 5′ upstream regulatory region of the mosquito Vg gene contains several binding sites for the ecdysone receptor EcR-USP complex and 20E-inducible genes. This pathway ensures that Vg production is tightly regulated and synchronized with the reproductive cycle, enabling the normal development of eggs following a blood meal. Specifically in *A. aegypti*, a blood meal stimulates Vg synthesis in the fat body by triggering the release of ovarian ecdysteroidogenic hormone (OEH) from the medial neurosecretory cells of the brain. OEH then activates the ovarian follicular cells to produce ecdysone, which is subsequently converted into the active hormone 20E in the fat body.

The research devoted to signal cascade in *D. melanogaster* has proven JH is capable of activating the expression of Met/Gce (Germ cell-expressed) and Kr-h1 in the dipterans, therefore inhibiting ecdysone biosynthesis in the prothoracic gland of *A. aegypti*, enhancing the function of EcR/USP in activating 20-inducible genes[30]. Conversely, JH signaling initiated at the cell membrane would bolster 20E production, amplifying the activity of EcR/USP in turning on genes inducible by 20E[30]. The homeostasis of 20E by JH pathways is still not well understood. The dual pathways of JH signaling are implicated in regulating ecdysone biosynthesis, thus coordinating the timing of 20E responses in different stages of insects, including *A. aegypti* [4]. This equilibrium is critical during its adult reproductive phase, where the PKC-induced phosphorylation of USP, which is activated through the membrane pathway, modulates 20E receptor function, thereby influencing the synthesis and action of 20E[23].

The confluence of JH's intracellular and membrane-associated pathways with the 20E signaling axis constitutes a robust regulatory network of *A. aegypti* 's lifecycle progression from follicle to adulthood. Environmental cues and nutritional status, notably the blood meal-induced vitellogenesis, tightly link these factors to the hormonal regulatory network. During this homeostasis, Kr-h1 stands as a cornerstone gene at the intersection of JH and 20E signaling, modulating its expression in response to these hormonal signals. In *Locusta migratoria*, Kr-h1 acts dually as a transcriptional repressor during molting and an activator in adult reproduction to dictate the insect's metamorphosis fate and reproductive capacity[43]. When Kr-h1 is upregulated by JH, the expression level of the downstream 20E-response gene would be downregulated. Deciphering the mechanism of Kr-h1 at a molecular level would offer a targeted approach for new vector control strategies.

1.5 Characteristics of Kr-h1 in Mosquitoes and Other Insects

Kr-h1 is a member of the zinc finger protein family distinguished by tandem modular, where eight instances are repeated in a series within a single protein molecule, Cys2-His2 (C2H2)-type zinc finger motifs that are consistently observed across various insect orders[42]. These motifs are composed of approximately 30 amino acids each, arranged in a loop stabilized by a zinc ion coordinated with cysteine and histidine residues, which is essential for DNA binding[42]. This configuration facilitates specific interactions with 20E-response gene segments, including E93, Br-C, and Spok, to regulate upcoming ecdysteriodogenesis (**Fig 5**). Comparative analyses of orthologous sequences across insect orders have confirmed the high conservation of the eight zinc-finger domains at the protein's very end of the C-terminus[39-41]. These additional regions have been identified as crucial for Kr-h1's role in transcriptional inhibition.

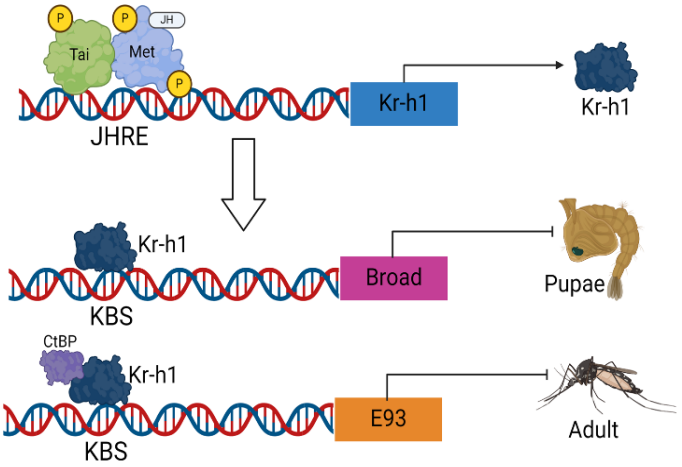

Figure 6. Kr-h1 regulation of Broad and E93 expression via JH-Met-Tai pathway. *JH complex binds to Juvenile Hormone Response Elements (JHRE) on the promoter, leading to the expression of TF Kr-h1. Kr-h1 binds to Kr-h1 binding sites (KBS) on target gene segments, inhibiting the expression of the pupal specifier Broad-complex (Br-C) and the adult specifier E93 to repress metamorphosis.*

Kr-h1 is indispensable in the physiological and developmental processes of insects. Except for metamorphosis and reproduction, Kr-h1 regulates the behavioral plasticity of insects, such as adjusting their flight behavior in response to various environmental stimuli, which is crucial for survival and effective host location[35]. Although *A. aegypti* are not eusocial, the role of Kr-h1 in caste differentiation in eusocial insects offers insights into its potential to affect social behaviors within mosquito populations. Kr-h1 is also instrumental in neuronal morphogenesis, guiding the development of neural circuits that govern essential behaviors like host-seeking and mating[36]. Furthermore, Kr-h1 is involved in sexual maturation, potentially regulating genes that affect the development of secondary sexual characteristics and mating rituals, such as the antennal responses of males to the wing-beat frequencies of females[37]. Moreover, Kr-h1 is integral to the metabolic regulation of *A. aegypti*, playing a key role in both lipid and carbohydrate metabolism. This regulation is mediated through its association with the Insulin/Insulin-like Growth Factor Signaling (IIS) pathway for lipid processing and influences carbohydrate management

through the Target of Rapamycin (TOR) pathway to respond to nutritional cues[38]. A multifaceted network of molecular pathways governs the expression of Kr-h1[24]. Additionally, post-translational modifications like histone acetylation and promoter methylation are key modulators to the Kr-h1 pathway, with evidence suggesting that such epigenetic alterations can regulate the expression of Kr-h1 or regulate ecdysone-related TFs Spok through Kr-h1 binding and vice versa[24] (**Fig 5**).

1.6 The Dual Role of Kr-h1 and Potential Interactions with KAPs

Our previous research has revealed Kr-h1's complex role in mosquito reproduction. It functions as both a transcriptional activator and repressor depending on the promoter sequence of target genes[44]. The study demonstrated that Kr-h1 is upregulated by JH in newly emerged adult mosquitoes, with its protein levels peaking at 48h PE and decreasing significantly after a blood meal, coinciding with JH expression profile. The RNAi-mediated depletion of Kr-h1 substantially reduced egg production post-blood feeding. Chromatin Immunoprecipitation (ChIP) experiments identified several in vivo binding sites of AaKr-h1 in the fat body of previtellogenic female mosquitoes.

However, despite AaKr-h1 binding to six genes similarly in the previtellogenic stage, their expression displayed two distinct patterns. The mRNA levels of AAEL005810, AAEL013177, and AAEL005957 increased 1.8–2.5 fold after eclosion, peaking at 48h PE, then gradually decreased, reaching the lowest levels at 12h PB. On the other hand, the expression of AAEL014226, AAEL004444, and AAEL005545 showed a different pattern compared to the mRNA profile of AaKr-h1[44]. Their mRNA levels decreased after adult emergence, reaching the lowest amounts at 48 hours post-eclosion (PE), and then gradually increased. This lowest expression at 48h PE coincided with the maximal binding of AaKr-h1 to the regulatory regions of these genes. These expression profiles correlated well with the mRNA profile of AaKr-h1. All the upregulated and downregulated genes were associated with multiple functional categories. RNAi experiments showed that depletion of Kr-h1 led to significant but variable changes in the expression of these target genes. For example, Kr-h1 depletion upregulated AAEL005545 and AAEL004444 but downregulated AAEL005957 and AAEL013177, indicating gene-specific regulatory roles[44].

This duality is crucial for the transcriptional response to the JH pathway in adult *A. aegypti*, influencing vital reproductive processes like previtellogenesis, vitellogenesis, and oogenesis. Modulating the activity of AaKr-h1 is essential for the temporal regulation of gene expressions that are necessary for follicle growth and oviposition. Since Kr-h1 could upregulate several genes while downregulating others

simultaneously and C2H2 zinc finger domains can also associated with various protein-protein interactions, it is reasonable to speculate that, in addition to binding specific DNA sequences, the eight C2H2 zinc finger domains of Kr-h1 are also capable of associate with other TFs in *A. aegypti*[48]. Because of the interaction between AaKr-h1 and AaKr-h1 associated proteins (AaKAPs), AaKr-h1 would form multiple complexes to recruit various cofactors to regulate the expression levels of downstream JH-response genes.

To verify the hypothesis, this research delves deeper into the molecular interactions that underpin Kr-h1's regulatory functions. Despite the known roles of Kr-h1, the specific potential interactions between Kr-h1 and other transcription factors (TFs), as well as its differential effects on target gene expression remain poorly understood. This study aims to fill this significant gap by elucidating whether Kr-h1 interacts with other TFs contribute to its essential roles in the physiological processes of mosquitoes.

By clarifying these mechanisms can enhance our understanding of mosquito reproductive physiological pattern and open novel avenues for developing highly specific control strategies that disrupt mosquito reproduction without affecting non-target organisms. Our study aims to provide detailed insights into the transcriptional networks regulated by Kr-h1, offering new perspectives on the modulation of gene expression in response to hormonal cues in mosquitoes[117-118].

1.7 Identification and Functional Analysis of KAPs

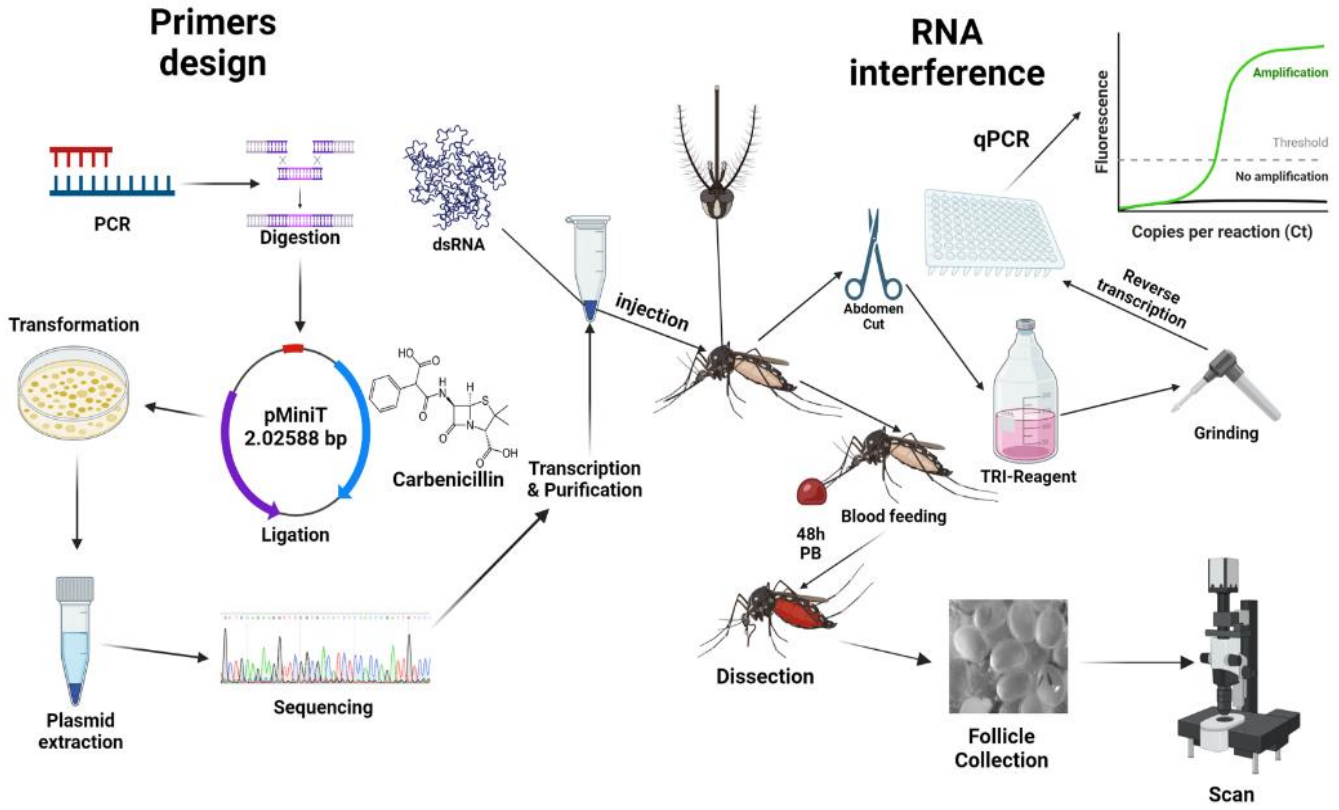

Figure 7. Comprehensive Process from Primer Design to Confirmation of KAP Function in A. aegypti. *Custom primers are used for PCR amplification of target DNA, followed by digestion, ligation into the pMiniT 2.0 vector, transformation into E. coli, incubation, plasmid extraction, and sequencing. Confirmed plasmids are transcribed and purified to produce high-concentration dsRNA. Adult female mosquitoes are injected with dsRNA, followed by abdomen cut and grinding in TRI-reagent. Residue fed with blood. At 48 hours post-blood feeding, mosquitoes are dissected to collect vitellogenic follicles for length comparison. The analysis includes qPCR for transcript levels and assessment of the impact on reproduction.*

To delineate the molecular mechanism between Kr-h1 and potential KAPs, the yeast two-hybrid (Y2H) system was used to identify potential KAPs. In this assay, Kr-h1 served as the bait protein, fused to the DNA-binding domain (DBD) of the yeast transcription factor GAL4, and potential KAP candidates were fused to the transcription activation domain (AD) of GAL4. The interaction between Kr-h1 and any KAP facilitated GAL4 transcriptional activation to bind to the upstream activating sequences (UAS) of HIS3 reporter gene promoter, enabling HIS3 expression to support yeast growth on histidine-deficient media. The selection stringency was enhanced by the addition of 3-Amino-1,2,4-triazole (3-AT), an HIS3 enzyme inhibitor, to the medium. This setup ensured that only yeast cells exhibiting significant Kr-h1-KAP interactions could grow, effectively identifying relevant KAPs involved in DNA hybinding or chromatin remodeling.

Among dozens of candidates, three proteins stand out for their potential roles that can be involved in DNA transcription regulation and modification, acting as cofactors that interact with TFs and remodel histones

to influence gene expression. The first protein, zinc finger (ZnF), is notable for its capacity to mediate protein-protein interactions, featuring a SUF-4-like domain that binds to DNA and is associated with the recruitment of histone-lysine N-methyltransferase, which specifically methylates histone H3 at lysine 36 (H3K36). The second candidate, Mes-4, is a histone-lysine N-methyltransferase characterized by a SET domain, conferring it the ability to catalyze the methylation of H3-K36, a post-translational modification known to influence gene expression. Lastly, DP-1 functions as a dimerization partner for E2F transcription factors, playing a role in the methylation of histone H3 at lysine 9 (H3K9) and is essential for the process of oogenesis in flies, but its functionality in *A. aegypti* still need to be confirmed. These proteins represent potential candidates associated with Kr-h1 to influence gene regulation within the mosquito reproductive pathway.

1.8 Overview of Methodology and Significance

Our study is structured into three main objectives: Firstly, analyzing mRNA expression profiles of KAPs in the fat body of non-injected female mosquitoes at various stages post-eclosion and post-blood feeding. This will offer a baseline understanding of their transcriptional activity during critical reproductive phases. Secondly, to employ RNA interference (RNAi) to repress the expression of target KAPs and assess their specificity with the ΔΔ method of qPCR and WB, relative to the housekeeping gene RPS7, then compare the post-blood feeding follicle length to the control & wildtype groups (**Fig 7**). Thirdly, to implement Co-Immunoprecipitation (Co-IP) to validate the physical interactions between Kr-h1 and KAPs elucidating their cooperative role in the regulation of gene expression relevant to mosquito fecundity. We also aim to characterize the impact of KAPs on the expression of key reproductive genes, setting the stage for future work using CUT & RUN technology to map Kr-h1's genomic interactions with its associated proteins.

The interaction between Kr-h1 and KAPs advances the understanding of vitellogenesis in *A. aegypti*, which would offer a precise new target to disrupt mosquito reproduction. Unraveling the roles of KAPs within these pathways not only elucidates the complex molecular mechanisms governing mosquito fertility but also paves the way for designing insecticides that specifically target *A. aegypti*. Such targeted approaches promise to significantly diminish populations of this disease vector without adversely affecting other insect species, marking a critical step towards safer and more effective vector control methods. This specificity could revolutionize insecticide development, ensuring ecological balance while effectively combating vector-borne diseases.

Chapter 2: Functional Analysis of DP-1 in Mosquito Reproduction

2.1 Material and methods

2.1.1 Expression Profile Analysis

Fat bodies were harvested from *A. aegypti* females at specific intervals post-eclosion (0h, 48h, 72h) and post-blood meal (12h, 24h, 36h, 48h) with sterilized forceps. During dissection, fat bodies from three mosquitoes were pooled into one of four microcentrifuge tubes for each time point, with each tube containing 100 µL of TRI Reagent®. Immediately post-dissection, samples were placed on ice and then stored at -80°C to maintain RNA integrity. Upon completion of sample collection across all time points, samples were homogenized uniformly. To each sample, an equal volume of ethanol was added, and RNA was subsequently extracted using the Direct-zol™ RNA MicroPrep Kit, followed by DNase I treatment to eliminate potential DNA contamination.

Purified RNA was reverse transcribed into cDNA. For qPCR, each cDNA sample was distributed into three replicate wells on a 96-well plate with Luna® Universal qPCR Master Mix. Quantitative PCR was performed with specific primers for AaDP-1, AaZn-F, and AaSET, alongside RPS7 as the housekeeping gene for normalization. The relative expression levels were determined using the ΔΔCT method by subtracting the average ΔCT value of each sample from the control ΔCT value to compute fold changes in gene expression.

The mean fold induction for each treatment group was calculated from the results of the four replicate tubes, which corresponds to the original four tubes. These mean values were applied for the gene expression profiles (**Fig 11**). Standard deviations from the replicates were used as error bars to represent variability within the data.

2.1.2 Primer Design for RNAi

Primer sets were designed for the genes of interest to ensure specificity and efficacy in dsRNA synthesis. The initial selection of primer sequences utilized nucleotide BLAST searches to identify target specificity and mitigate off-target interactions. Afterward, NextRNAi software facilitated a refined design, optimizing the primers within RNAi libraries for enhanced specificity (**Fig 8**).

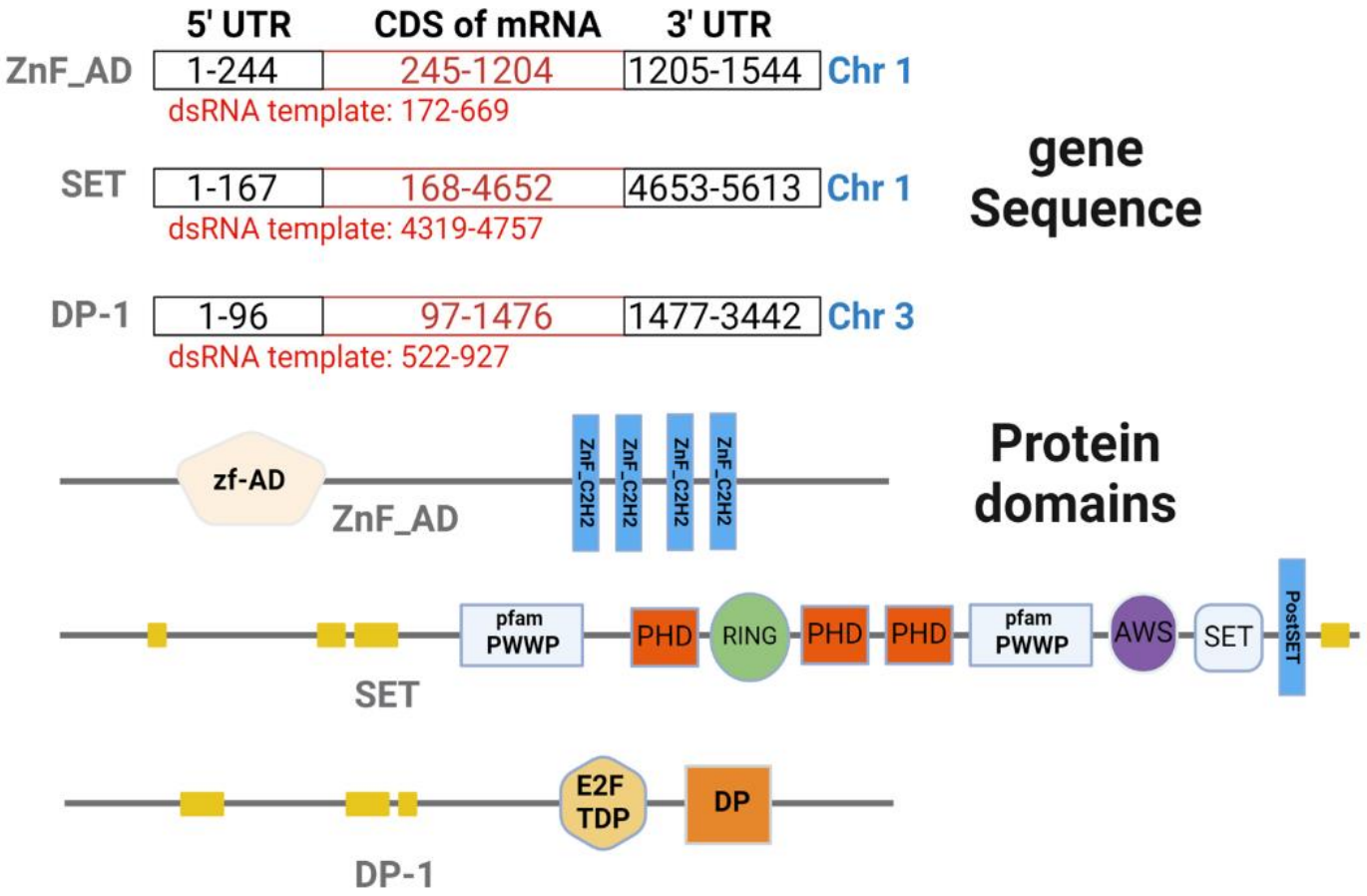

Figure 8: Gene Sequences and Protein Domains of three KAPs: ZnF_AD, SET, and DP-1 in A. aegypti*. For each protein, the 5' UTR, CDS, and 3' UTR regions are depicted alongside their respective dsRNA templates, with corresponding chromosomes indicated as Chr 1 and Chr 3. ZnF_AD contains a ZnF-AD domain mediating protein-protein interaction and multiple C2H2 zinc finger domains involved in DNA binding and recruitment of H3K36 methyltransferase. SET features PWWP, PHD, RING, AWS, and SET domains essential for histone methyltransferase activity (H3-K36 specific) and chromatin remodeling. DP-1 includes E2F-TDP and DP domains involved in histone H3-K9 methylation, dimerization with E2F transcription factors, and oogenesis in flies. This figure illustrates the potential roles of these KAPs in DNA transcription regulation and chromatin remodeling within Aedes aegypti.*

To allow the target sequences to be recognized by T7 RNA polymerase, a T7 promoter taatacgactcactataggg was added to the 5’ end. For the ZnF_AD gene, the forward primer sequence was determined as 5'-CGAACAGTTTGAAATTGACTCATC-3', comprising 24 nucleotides with a melting temperature (Tm) of 60.042°C and a GC content of 37.5%. The corresponding reverse primer was 5'-ATTGGTCTCTGGTTTCCTCTGAT-3', 23 nucleotides in length, with a Tm of 60.363°C and a GC content of 43.478%. The SET gene's forward primer was established as 5'-GCGAGGAGCTAACCTTCAACTAC-3', a 23-nucleotide sequence with a Tm of 60.771°C and a GC content of 52.174%, while its reverse counterpart was 5'-GCGTAGATTGCTGTTCTTCTTTG-3', also 23 nucleotides, with a Tm of 60.427°C and a GC content of 43.478%. Lastly, the primers for the DP gene included a forward primer 5'-TGCAGCAACCACAGTACAACTAC-3', 23 nucleotides long with a Tm of 60.281°C and a GC content

of 47.826%, and a reverse primer 5'-CCTTTCGTTTTCCTTCTCCAG-3', consisting of 21 nucleotides, a Tm of 60.220°C, and a GC content of 47.619%. Each primer pair underwent a penalty calculation to evaluate and minimize risks of self-complementarity and secondary structure formation, yielding penalty scores of 1.4044 for ZnF_AD, 1.1983 for SET, and 2.5012 for DP.

2.1.3 PCR Amplification and Ligation

PCR amplification utilized a BIO-RAD T100™ Thermal Cycler with a protocol initiating at 98°C for 30 seconds, followed by 35 cycles (98°C for 10 seconds, 53°C for 10 seconds, and 72°C for 30 seconds), concluding with a 72°C extension for 5 minutes with the reaction volume 50 µl. Post-amplification, products were purified using the **MinElute PCR Purification Kit**, adhering to manufacturer instructions, including a Buffer PB mix and column centrifugation. DNA was eluted with Buffer EB and verified by gel electrophoresis at 50V for 60 minutes. Next, the **MinElute Gel Extraction Kit** was employed to isolate specific DNA fragments from the gel. The target bands were excised under UV light, dissolved in Buffer QG, and loaded onto the MinElute column. Following the prescribed PE wash and centrifugation steps, the DNA was eluted with EB, and concentration was measured using a nanodrop spectrophotometer.

The purified DNA fragments were ligated to linearized pMiniT 2.0 vector using the **New England Biolabs ligation kit.** The ligation mix was incubated at 25°C for 15 minutes and on ice for 2 minutes before transformation into NEB 10-beta Competent *E. coli*.

2.1.4 Transformation and Colony Selection

Competent NEB 10-beta *E. coli* cells were transformed with recombinant plasmids and subjected to a precise heat shock at 42°C for 30 seconds to facilitate DNA uptake. The transformed *E. coli* were nurtured in Luria-Bertani (LB) medium for 1 hour to permit the expression of antibiotic resistance. This was followed by plating the cultures on LB agar plates with 100 ng/µl carbenicillin, and the plates were incubated at 37°C overnight. Under sterile conditions and with a flame from a Bunsen burner to ensure an aseptic environment, individual colonies were carefully selected with sterile toothpicks and transferred into flasks containing LB broth. The broth cultures were incubated at 37°C with continuous shaking at 225 rpm for 20 hours, facilitating bacterial proliferation and plasmid propagation. The extraction and purification of plasmid DNA were carried out using the **QIAprep Spin Miniprep Kit** followed by spin column purification. The final elution step was performed with the provided Buffer EB and the concentration of the purified plasmid was assessed using a Nanodrop spectrophotometer.

2.1.5 Plasmid Verification

Extracted plasmids were digested with EcoRI-HF and incubated at 37°C for enzymatic reaction, followed by heat inactivation. Digestion was confirmed on a 1.2% agarose gel (**Fig 10**). Selected colonies were sent for Sanger sequencing to verify primer specificity and cloned target sequence. For each sequencing reaction, 1 µg of the respective purified plasmid was combined with 1 µL of primer (3.2 pmol/µL concentration), and the total volume was adjusted to 10 µL with the addition of water and sequenced using standard capillary electrophoresis.

2.1.6 Target dsRNA Production

After confirming successful digestion, the plasmid DNA was diluted to 1 ng/µL and used as the template for PCR. The PCR was performed using the **Platinum™ SuperFi™ II PCR Master Mix Kit**, with a total reaction volume of 50 µL comprising 25 µL of biomix, 5 µL each of forward and reverse primers, 14 µL of nuclease-free water, and 1 µL of template DNA. The amplification was carried out in a **T100™ Thermal Cycler**. Following PCR, the concentration and purity of the amplified DNA were assessed using a Nanodrop spectrophotometer. A 1.2% agarose gel electrophoresis was then conducted to verify the size and purity of the DNA, ensuring its suitability for subsequent RNA transcription (**Fig 17**).

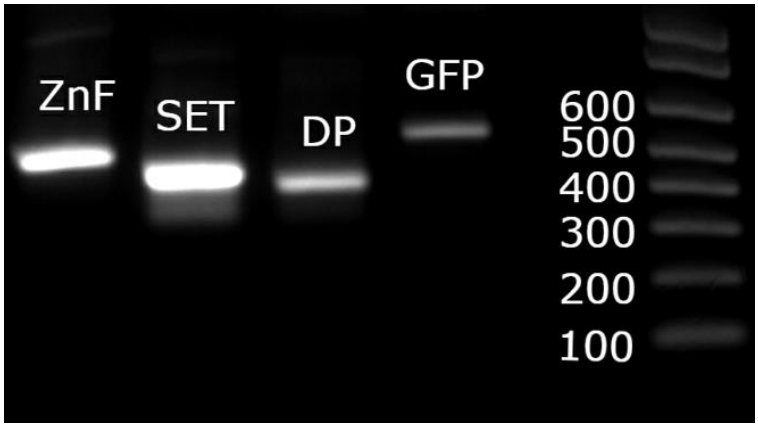

Figure 9. Agarose Gel Electrophoresis of PCR Amplifications. *Lane 1: ZnF_AD gene amplicon expected size 498 bp. Lane 2: SET domain-containing protein (SET) gene amplicon, expected size 441 bp. Lane 3: DP gene amplicon, expected size 404 bp. Lane 4: GFP control amplicon. Lane 5: DNA ladder with marker sizes indicated on the right, in base pairs (bp). The bands verify the expected sizes of the amplified products.*

HiScribe T7 Quick High Yield RNA Synthesis Kit was used to synthesize dsRNA following a modified protocol for enhanced yield. A Standard 20 µl reaction is anticipated to yield approximately 180 µg RNA from a 1 µg DNA template. An 80 ul scale-up reaction was established for each target gene.

When RNA synthesis was complete, reactions were diluted with 30 µl of DEPC-treated water per original 20 µl reaction and subjected to a denaturation step at 75 °C for 5 minutes, consequently allowed to naturally cool to approximately 35 °C. To remove the DNA template, 2 µl of DNase I was added per original 20 µl reaction volume, mixed, and incubated for an additional 15 minutes at 37 °C.

RNA purification was performed using the **Monarch RNA Cleanup Kit** (New England Biolabs), with the precaution that RNA binding capacity for each column is capped at 500 µg. This necessitated the use of multiple columns for binding when the reaction exceeded this threshold. During the elution phase, 100 µl of DEPC-treated water was applied to the column and allowed to incubate for 5 minutes, followed by a gentle resuspension of the column contents. After a secondary 5-minute incubation, the column was centrifuged to collect the eluted RNA. A second elution step was repeated with an additional 100 µl of DEPC-treated water to ensure maximal recovery.

After combining eluates, the total volume was quantified, with a small aliquot reserved for concentration determination via Nanodrop. RNA precipitation was facilitated by adding 1/10th volume of 3 M sodium acetate (pH 5.2) and 1 volume of room temperature 100% isopropanol, followed by overnight incubation at -20 °C. RNA was then pelleted by centrifugation at 13,200 rpm for 30-60 minutes at 4 °C. The supernatant was aspirated with the pipette, and the RNA pellet was washed with 1 ml of 70% ethanol, rested for 5 minutes, and re-centrifuged at 13,000 rpm for 30-60 minutes at 4 °C. Following supernatant removal, the RNA pellet was air-dried for 15 minutes and then resolubilized in a specialized saline solution formulated for *Aedes* species (*Aedes* physiological saline APS), composed of 150 mM NaCl, 4 mM KCl, 1 mM CaCl2, 0.1 mM NaHCO3, 0.6 mM MgCl2, and buffered with 25 mM Hepes at pH 7.0. Final RNA concentrations were adjusted to 5-6 µg/µl based on the Nanodrop readings.

2.1.7 Rearing Conditions of *A. aegypti*

Laboratory colonies of *A. aegypti* (Liverpool strain) were reared under controlled environmental parameters with a temperature set at 28 °C and relative humidity maintained between 60% and 70%. The photoperiod was regulated to mimic a natural light cycle, with 14 hours of light followed by 10 hours of darkness. Larval mosquitoes received a diet of finely pulverized TetraMin Tropical Flakes, ensuring optimal growth conditions. Adult insects had constant access to a 10% sucrose solution (weight/volume), delivered via a cotton wick immersed in a solution-filled container. The sucrose cotton was renewed every 3 days to avoid starvation and contamination. Female mosquitoes, aged between 5 to 7 days post-emergence (PE), were provided a defibrinated sheep blood meal for a duration of 20 to 30 minutes to stimulate the vitellogenesis and oviposition process. Dissection procedures were carried out in APS to closely replicate the mosquitoes' internal ionic environment.

2.1.8 The dsRNA injection into *A. aegypti*

Post-eclosion female *A. aegypti* were subjected to RNA interference (RNAi) via microinjection of synthesized dsRNA. Prior to injection, mosquitoes were briefly cooled at 4°C and then immobilized on an ice-cold Petri dish (**Fig 10**). Using a micromanipulator, 400 nL of concentrated dsRNA (5 µg/µl) was injected into each mosquito at a rate of 60 nL per second, targeting the area adjacent to the three white dots on the thorax. For control groups, the same volume of GFP dsRNA (5 µg/µl) was injected to serve as a negative control to account for any effects caused by the injection process itself. Additionally, a wild-type group was maintained to ensure the baseline normalcy of the experimental mosquito population.

Figure 10: Immobilized post-eclosion female Aedes aegypti on ice*. Female mosquitoes were chilled and immobilized on an ice-cold Petri dish for RNAi microinjection procedures.*

2.1.9 RNA Extraction and Purification

Following dsRNA administration, male *A. aegypti* were introduced to female groups at a ratio of 1 male to 1-2 females for mating. Six days PE, females from each group were dissected to collect abdomens. Each abdomen was placed in microcentrifuge tubes with 100 µL of TRI Reagent; experimental samples contained one abdomen per tube, while control samples (GFP and wildtype) had three in each tube. Tissues were homogenized using a pestle motor, with an additional 300 µL of TRI Reagent® added, followed by vortexing and overnight storage at 4°C.

RNA extraction involved adding 400 µL of ethanol to each sample, then transferring the mixture to Zymo-Spin™ IC Columns for DNase I treatment to eliminate genomic DNA. Following wash steps with Direct-zol™ RNA PreWash and RNA Wash Buffer, RNA was eluted in 21 µL of DNase/RNase-Free Water. RNA concentration and purity were determined via Nanodrop spectrophotometer. Residual DNA was removed via 1 µL DNase I treatment in DNA digestion buffer at room temperature for 15 minutes. DNase I was deactivated by adding 1 µL of 25 mM EDTA to the digestion, and heating at 65°C for 10 minutes. The RNA was then ready for reverse transcription and PCR amplification.

2.1.10 Reverse Transcription and Quantitative Real-Time PCR (qPCR) Analysis

The cDNA was synthesized from RNA extracts utilizing the **LunaScript® RT Master Mix Kit (Primer-free)** from New England Biolabs. The reaction setup comprised 2 µl of d(T)23 VN primer (50 µM), 4 µl of 5X LunaScript RT Master Mix, 1 µg of RNA, adjusted to a total volume of 20 µl with nuclease-free water. The procedure initiated with a 2-minute primer annealing at room temperature, followed by a 10-minute cDNA synthesis at 55°C, and concluded with a 1-minute heat inactivation at 95°C on a BIO-RAD PCR Thermal Cycler. For qPCR, cDNA samples were diluted with 30 µl of nuclease-free water.

qPCR was performed on the CFX Opus 96 Real-Time PCR System using clear Multiplate PCR Plates (96-well). The reaction, totaling 20 µl, included 10 µl of 2X Luna Universal qPCR Master Mix, 0.5 µl of 10 µM forward and reverse qPCR primers, and 2 µl of cDNA, topped up with nuclease-free water. The cycle began with a 95°C denaturation for 60 seconds, followed by 40 cycles of denaturation at 95°C for 15 seconds and annealing/extension at 65°C for 30 seconds. A melt curve analysis from 60°C to 95°C assessed amplification specificity. Each sample underwent triplicate assays to ensure consistency. RPS7 gene served as a normalization reference, with the ΔΔCT method applied for relative gene expression evaluation, delineating the efficiency of gene silencing.

2.1.11 Protein Extraction and Quantification from *A. aegypti* Abdominal Tissue

Abdominal tissues from 6 days PE female *A. aegypti* were collected for protein analysis. Five abdomens per group, including GFP and wildtype controls, were pooled into four replicates and quickly frozen in liquid nitrogen. Each sample was lysed with 100 µL of Pierce IP Lysis Buffer and 1 µL of a 100X protease and phosphatase inhibitor cocktail. Homogenization was performed using a motorized pestle, followed by a 10-minute incubation at 4°C and centrifugation at 13,000 rpm for 10 minutes at 4°C to remove cellular debris. The clear supernatant was transferred to new tubes.

Protein concentration was determined using the Pierce Detergent Compatible Bradford Assay. A 10 µL aliquot of each supernatant was mixed with 1.5 mL of Bradford reagent, and after 10 minutes at room temperature, absorbance was measured in a spectrophotometer.

2.1.12 Western Blotting for Protein Expression Analysis

For Western blot analysis, equal volumes of proteins (up to 16 µL) from each sample were mixed with 20 µL of Tris-glycine SDS sample buffer (2X) and 4 µL of sample reducing agent (10X), adjusting the final volume to 40 µL with nuclease-free water. Samples were denatured by heating at 85°C for 2 minutes, then briefly centrifuged to collect the liquid at the bottom of the tubes.

Proteins were separated via SDS-PAGE by loading 40 µL of each sample into the wells of a 4-20% tris-glycine gradient gel and adding a protein ladder to the final well for molecular weight reference. Electrophoresis was performed at 200 V for 60 minutes. The separated proteins were then transferred onto a nitrocellulose membrane using a wet transfer system set at 25V for 120 minutes.

The membrane underwent blocking in 5% non-fat dry milk in PBST (Phosphate-Buffered Saline with 0.05% Tween 20) for one hour at room temperature to minimize non-specific adsorption. Primary antibodies for DP were applied at a 1:600 dilution in blocking buffer and left to bind for over four hours at room temperature with mild shaking. The membrane was then cleansed four times with PBST, five minutes per wash, to remove unbound antibodies.

Next, a secondary antibody tagged with horseradish peroxidase, diluted to 1:100,000 in blocking buffer, was introduced and incubated for an hour under mild agitation. Afterward, the membrane was subjected to four additional PBST washes. For detection, a mix of SuperSignal West Dura Luminol/Enhancer and Stable Peroxide (1:1 ratio) was employed, enveloping the membrane for 5-10 minutes before imaging on an Azure 200 gel imager. Band intensities were scrutinized to appraise the differential expression of target proteins.

2.1.13 Follicle Length Assessment to Determine RNAi Impact on Mosquito Reproduction

To discern the phenotypic consequences of RNAi on *A. aegypti*, an analysis of follicle length post-blood meal was conducted. Following a feeding 6-day PE on sheep blood, female mosquitoes from each experimental and control group were dissected at 24 to 48 hours after blood feeding. Utilizing phosphate-buffered saline (PBS) for the procedure, ovaries were carefully extracted using fine-tip forceps and prepared on microscope slides for subsequent examination.

Imaging of the dissected follicles was taken with the fluorescent microscope, enabling the precise documentation of follicle length variations across the differentially treated groups. ImageJ software facilitated the quantitative measurement of follicle lengths, utilizing pixel counts as the primary unit of measurement. These pixel counts were then converted into millimeters to standardize the data across all samples. The compiled measurements were analyzed using RStudio to generate scatter plots, offering a visual comparison of follicle length discrepancies among the groups.

2.1.14 Egg Production and Hatching Rate Evaluation

Following dsRNA treatment, the fecundity and hatching viability of *A. aegypti* were assessed to gauge the impact of RNA interference on mosquito reproduction. Female mosquitoes were housed in individual oviposition chambers maintained at 28°C, 60-70% humidity, and subjected to a 14-hour light/10-hour dark cycle. After a 72h blood meal, the eggs laid on moistened oviposition paper within each chamber were diligently photographed. The photographs served to accurately count the eggs, with the resulting data presented in scatterplot graphs to illuminate the influence of dsRNA on egg laying patterns.

2.1.15 Preparation of Expression Vectors for Recombinant Proteins

To investigate the interaction between TF DP-1 and Kr-h1, their coding sequences were separately cloned into expression vectors, specifically pAc5.1A for DP-HA and pAc 5.1B for Kr-h1-myc, incorporating epitope tags for protein identification. Following cloning, the constructs were introduced into *E. coli* cells competent for transformation with heat shock at 42°C for 30s. Transformed cells were then selected based on their resistance to carbenicillin and propagated in the LB medium. After sufficient growth, plasmids were harvested from the bacterial cultures. The concentration and purity of the extracted plasmids were assessed with a Nanodrop spectrophotometer, while the integrity of the constructs was verified by agarose gel electrophoresis.

2.1.16 Cell Culture and Transfection

Aedes aegypti Aag2 cells were cultured in 2 mL Schneider's Drosophila Medium (1X) at room temperature (**Fig 18**). Before transfection, cells were seeded in 6-well plates at a density ensuring overnight attainment of over 80% confluency. Transfections were carried out using 2 µg of plasmid DNA (1:1 ratio of Kr-h1 to DP for experimental groups and 2 µg of DP plasmid for control) mixed with 4.5 µL FuGENE HD Transfection Reagent per well. After transfection, cells were incubated overnight, followed by a medium change to minimize transfection reagent toxicity.

2.1.17 Co-Immunoprecipitation (Co-IP) Assay

Aag2 cells were lysed using the **Pierce™ Direct Magnetic IP/Co-IP Kit**. The lysate was prepared by washing cells with PBS, lysing with IP Lysis/Wash Buffer, and clarification by centrifugation. Antibody specific to myc was coupled to NHS-Activated Magnetic Beads and mixed with cell lysates to bind the recombinant myc-Kr-h1protein. Following incubation, beads were washed, and bound proteins were eluted. The eluted proteins were subjected to Western Blotting to verify DP and Kr-h1 interactions.

2.1.18 The mRNA Expression Profiling in Mosquito Fat Body

Fat bodies were excised from *A. aegypti* at intervals of 24h PE and at 12-hour increments following blood meals. Each dissection focused on preserving the integrity of the fat body while excluding other abdominal contents.

For quantitative PCR analysis, mRNA levels of Kr-h1, DP, Zn-F, and SET were evaluated. The cDNA synthesized from extracted RNA served as the template for qPCR, with RPS7 as the internal standard for normalization. The resulting expression profiles, reflective of gene activity across the various time points, were systematically tabulated and graphically presented to depict the temporal regulation of gene expression within the mosquito fat bodies.

2.2 Result

2.2.1 Expression of Potential KAPs in the Fat Body of Adult Female *A. aegypti* Mosquitoes

The qPCR results revealed distinct patterns of mRNA expression for the target genes across different stages of mosquito development (**Fig 11**). AaDP-1 exhibited a notable increase in transcript levels 12 hours post-blood meal, peaking sharply compared to other time points. This suggests a significant role of AaDP-1 during early vitellogenesis. In contrast, AaZn-F displayed minimal expression throughout the stages, indicating either a non-critical role during these specific periods or its involvement in other physiological processes not captured in this study. AaSET expression showed a modest increase during the initial stages of the vitellogenic phase, subtly rising post-eclosion and maintaining slightly elevated levels through the early post-blood meal phase. This pattern suggests a potential regulatory role in early vitellogenesis but is not as pronounced as AaDP-1.

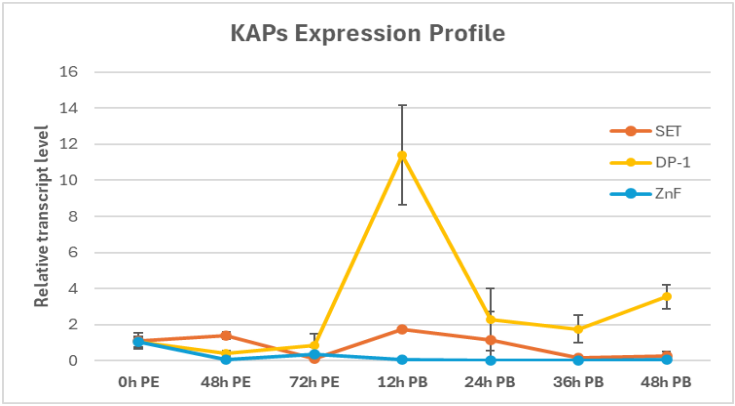

Figure 11. Temporal expression dynamics of selected potential Kr-h1 interacting proteins (KAPs) in the fat body of Aedes aegypti during the previtellogenic and vitellogenic stages*. mRNA levels of AaDP-1, AaZn-F, and AaSET were quantified at various times post-eclosion (PE) and post-blood meal (PB) using quantitative real-time PCR. The graph represents mean expression levels ± standard deviation (SD) across three biological replicates. PE denotes the period following eclosion; PB denotes the period following a blood meal.*

2.2.2 Confirmation of Effective DNA Ligation and Primer Specificity

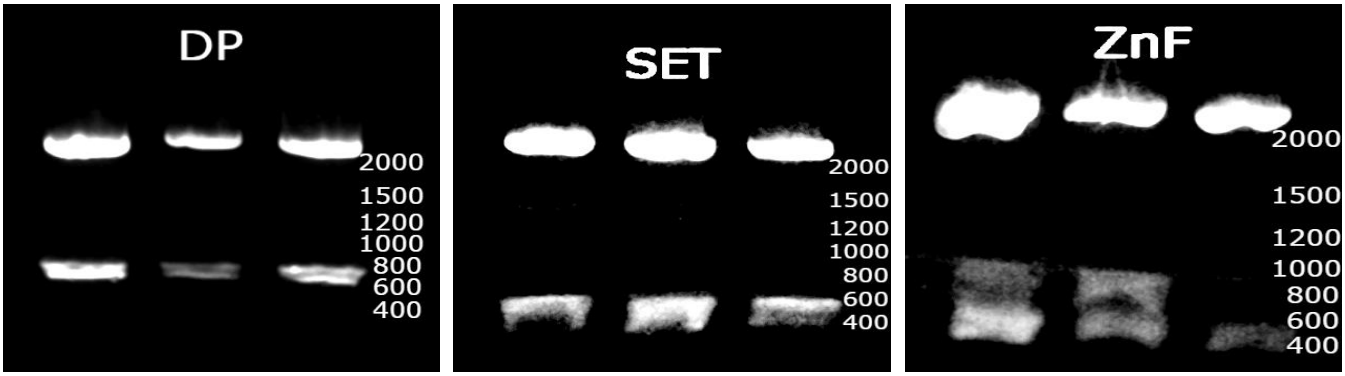

Figure 12. Restriction Digest Verification of Plasmid Inserts for A. aegypti. *The images show the results of EcoRI-HF digestion of vector pMiniT 2.0 containing inserts for the genes DP-1, SET, and ZnF_AD, run on a 1.2% agarose gel. For each gene, the upper band represents plasmid DNA, and the lower band(s) indicate the presence of specific fragments post-digestion.*

The appearance of two distinct bands on the gel (**Fig 12**) following EcoRI-HF digestion indicates effective ligation of DNA fragments into the **pMiniT 2.0 vector**, confirming the specificity of the custom-designed primers. This underpins the subsequent results from mosquitoes injected with the corresponding dsRNA, ensuring the reliability of the downregulation effects observed.

2.2.3 AaDP is Required for Egg Production During the Vitellogenesis of A. aegypti

To investigate the role of AaDP-1 in egg production, the expression of AaDP-1 was repressed by RNA interference (RNAi) (**Fig 13**). Following the purification and precipitation of dsRNA, the samples were subjected to 1.2% agarose gel electrophoresis to confirm their purity and verify their expected base pair sizes (**Fig 14**). The electrophoresis results demonstrated that the synthesized dsRNA constructs for target samples were pure, devoid of template DNA, and correctly sized, indicating successful

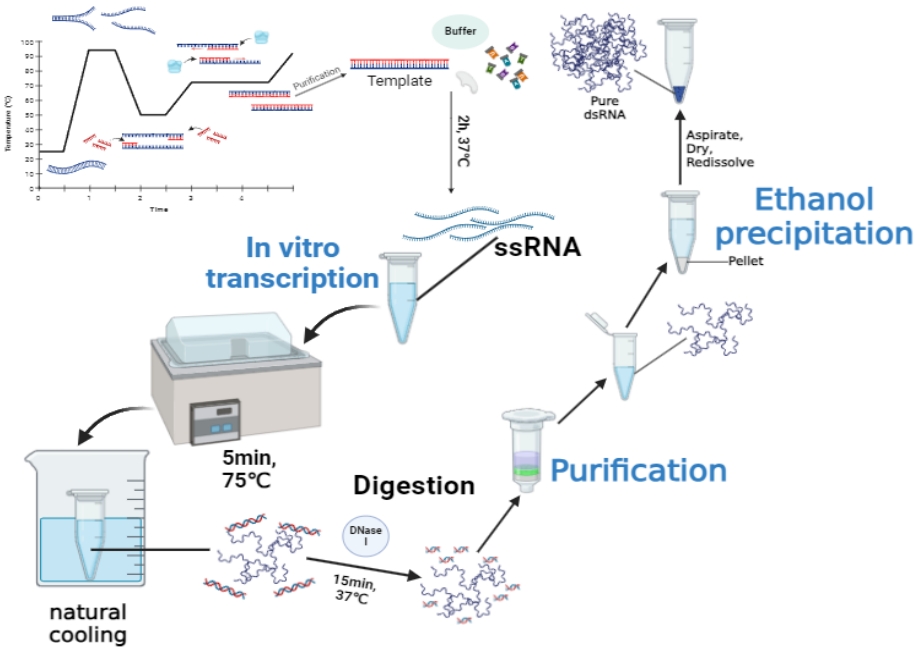

Figure 13. dsRNA Synthesis for Mosquito Injection. *The KAP DNA is PCR amplified, purified, and transcribed with T7 RNA polymerase at 37°C for 2 hours. The RNA is heated to 75°C for 5 minutes and naturally cooled to form dsRNA. DNase I treatment at 37°C for 15 minutes removes the DNA template. The dsRNA is purified with a silica column, precipitated with sodium acetate and isopropanol, washed with 70% ethanol, dried, and resuspended in ASP for mosquito injection.*

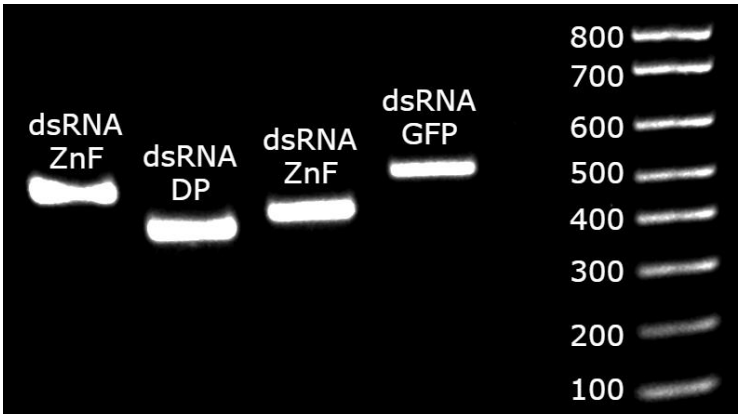

Figure 14. Agarose gel electrophoresis of purified dsRNA constructs. The lanes contain dsRNA for ZnF, DP, and GFP, respectively*. The rightmost lane shows the 100bp DNA ladder with marker sizes indicated in base pairs (bp).*

synthesis and preparation for RNAi experiments. Newly emerged adult female mosquitoes received injections of either AaDP-specific double-stranded RNA (dsRNA) or control green fluorescent protein (GFP) dsRNA around 1.5h PE, with a third group serving as the wildtype group. The effective knockdown of AaDP-1 was verified through real-time PCR (**Fig 15**) and WB analysis (**Fig 19B**). RNAi effectively reduced AaKAPs levels in adult female *A. aegypti* injected with their corresponding target dsRNA compared to the GFP control and the wildtype group. All females were adequately mated with age-matched males at 96h PE to ensure oocyte fertilization. At 120h PE, the transcription levels of AaKAPs were quantified in one individual from the dsRNA KAPs injected group and compared with three randomly selected individuals from the dsRNA GFP injected and uninjected cohorts. The real-time PCR data, which is presented as the mean ± standard deviation (S.D.) from triplicate assays,

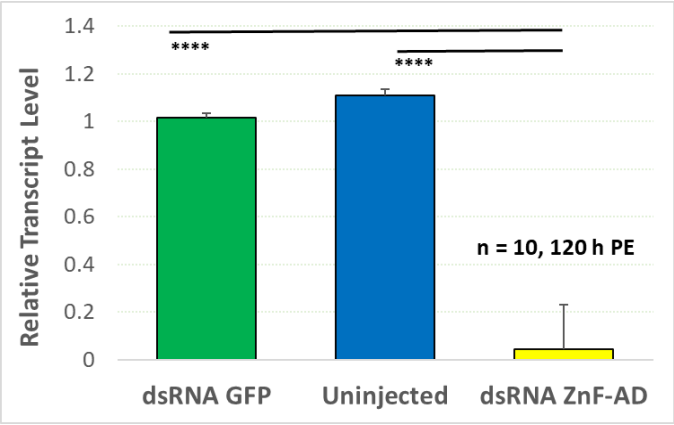

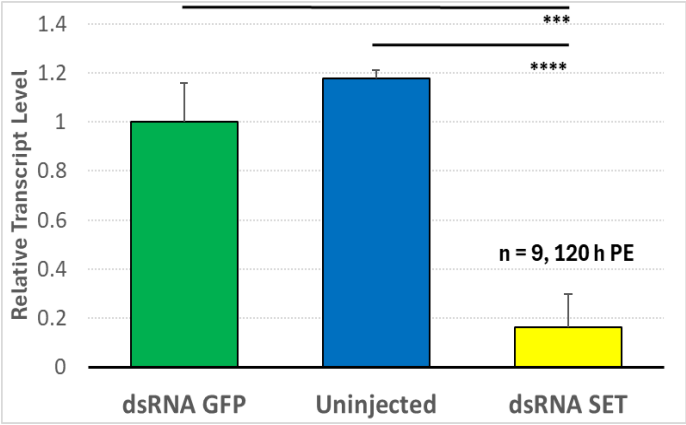

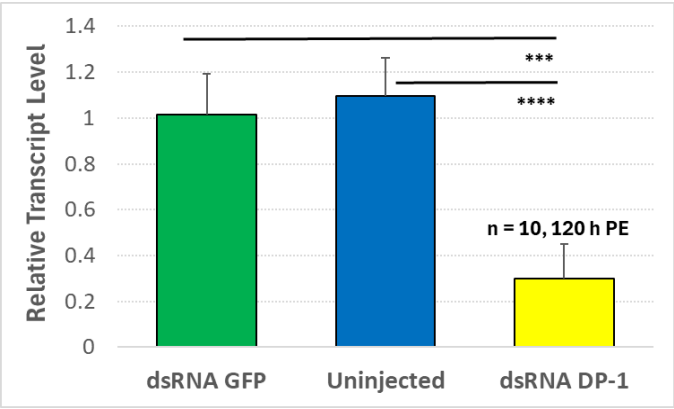

Figure 15. Quantitative PCR (qPCR) Analysis of Relative Transcript Levels of Potential Kr-h1 Associated Proteins (KAPs) ZnF, SET, and DP in A. aegypti. *Relative transcript levels of the target genes ZnF, SET, and DP were measured using qPCR and represented using the ΔΔCT method. Each bar represents the mean relative transcript level ± standard deviation (SD) at 120 hours post-eclosion (PE). The yellow bars indicate the dsRNA-treated groups (ZnF, SET, DP), the blue bars represent the wildtype groups, and the green bars denote the GFP-injected control groups. Sample sizes were n = 10 for ZnF and DP, and n = 9 for SET. Significant differences in relative transcript levels are indicated with p-values (p < 0.001 represents with *** and p < 0.0001 represents with ****).*

underwent paired t-test analysis. This statistical analysis demonstrated significant downregulation of the target genes, as indicated by the small p-values, confirming the efficacy of the RNAi treatment in knocking down AaDP-1 expression and its associated effects on gene expression (**Fig 15**).

Transcriptomic modifications identified through RNA-seq analyses were consistent with the phenotypic variations observed in follicle length alterations. Six days post-injection, female mosquitoes from the wild type, dsGFP-injected, and dsDP-injected groups were fed defibrinated sheep blood. 24h and 48h post-feeding, the follicle lengths were measured using ImageJ software respectively, and the number of eggs laid by each female was manually counted (**Fig 16-17**). The data were subsequently analyzed using RStudio software (**Fig 18**). The preliminary analysis revealed that mosquitoes injected with dsDP exhibited a 33.3% reduction in follicle length and a 31.6% decrease in egg production compared to the dsGFP-injected group ($p<0.001$). However, there were no significant differences in follicle length between the wild-type and dsGFP-injected controls ($p>0.1$). These findings suggest that AaDP is crucial for the repro ductive processes regulated by Kr-h1 in *A. aegypti*.

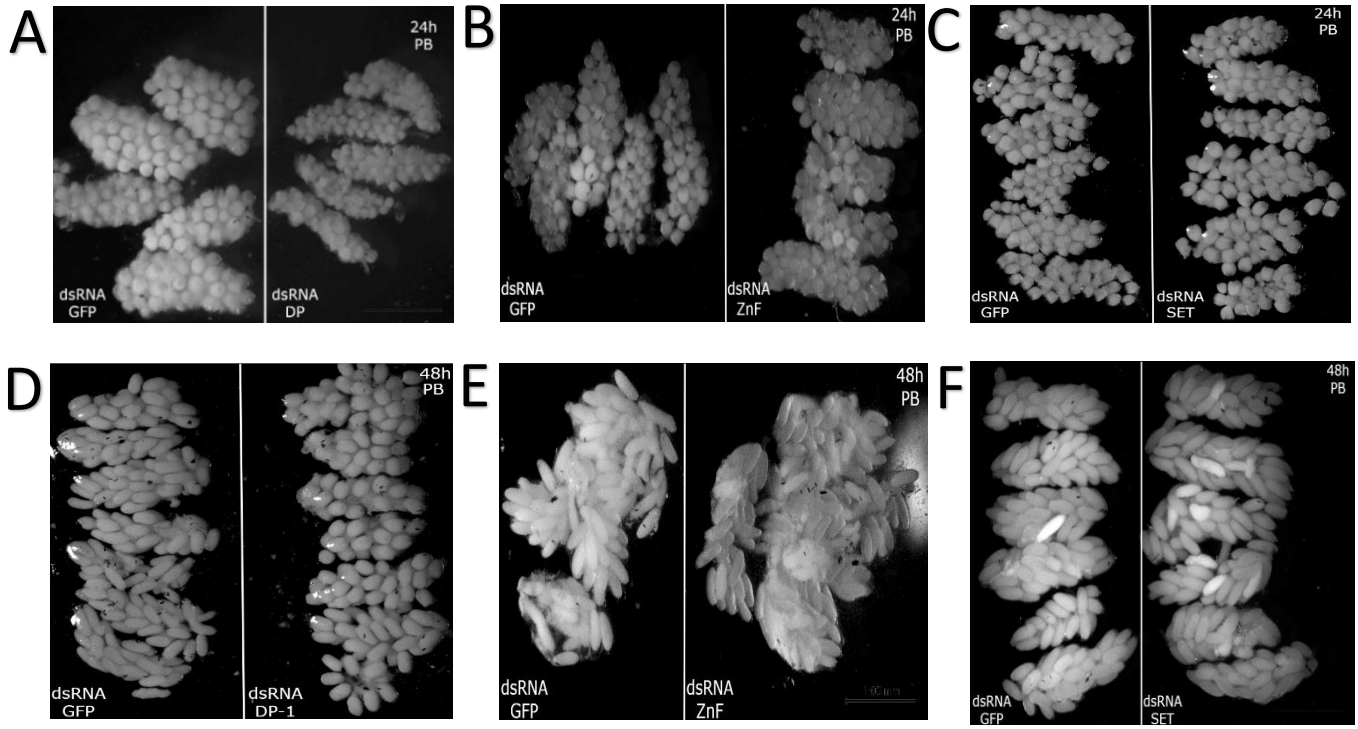

Figure 16. Impact of dsRNA Treatment on Ovarian Follicle Development in A. aegypti. *Adult female mosquitoes were dissected at 24- and 48-hours post-blood meal (PB) to evaluate the effect of dsRNA on ovarian follicle development. Females were injected with purified dsRNA targeting specific genes—GFP (as control), DP-1, ZnF_AD, and SET—at concentrations ranging from 5,000 ng/µL to 6,000 ng/µL. Follicles are visualized as semi-transparent white structure. At both 24h and 48h PB, follicles in the DP-treated group were significantly smaller compared to those in the GFP control group. Conversely, the follicles in the ZnF_AD and SET-treated groups did not exhibit significant size variations from the control at these time points.*

The protein levels of AaDP were assessed in the abdomens of adult female mosquitoes to further examine the effects of RNA interference (RNAi). Protein extracts from wild-type, dsRNA GFP-treated, and dsRNA DP-treated *A. aegypti* were subjected to immunoblotting using an anti-rabbit-DP antibody. The expected protein size was 50 kDa (**Fig 19B**). Intensities from the DP-treated lanes (DP1–DP4) were normalized

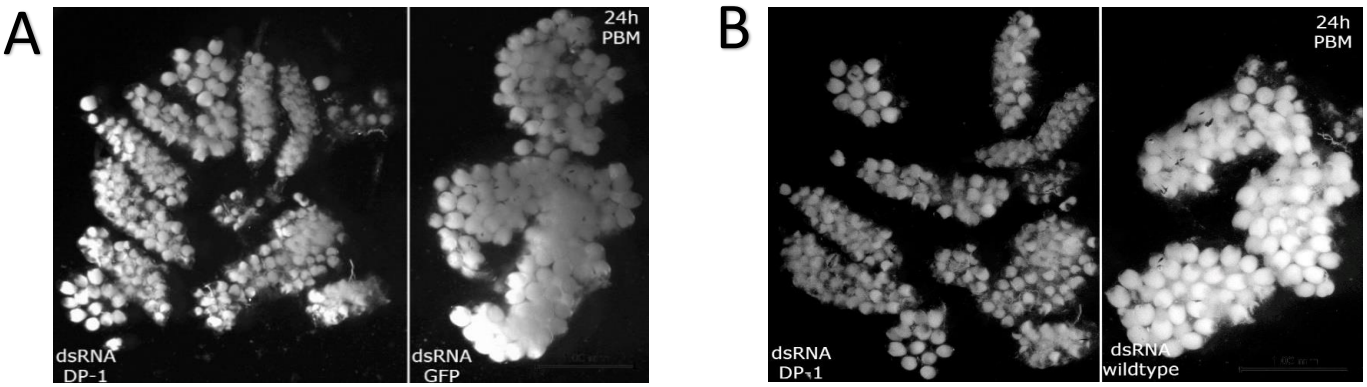

Figure 17. Further Comparative Analysis of Follicle Development in dsRNA DP-1 Injected A. aegypti at 24h PBM. (a) *The comparison of ovarian follicles between dsRNA DP-1 injected (left), dsRNA GFP injected (right), at 24 hours post-blood meal (PBM). The follicles in the DP-1 group show a marked reduction in size compared to the GFP and wildtype groups.* ***(b)*** *he comparison of ovarian follicles between dsRNA DP-1 injected (left), wildtype group (right). The follicles in the DP-1 group also show a obvious smaller size compared to the GFP and wildtype groups.*

against the GFP1 control. Analysis showed that when each tube contains 5 abdomens from mosquito, two out of four samples from the dsRNA DP1-injected group exhibited a significant reduction in AaDP expression. This obvious decrease of chemiluminescence intensity in the DP lanes indicates a successful knockdown of AaDP protein levels due to the dsRNA treatment.

Recombinant Kr-h1 and DP were each tagged with myc and HA tags respectively and expressed in *A.*

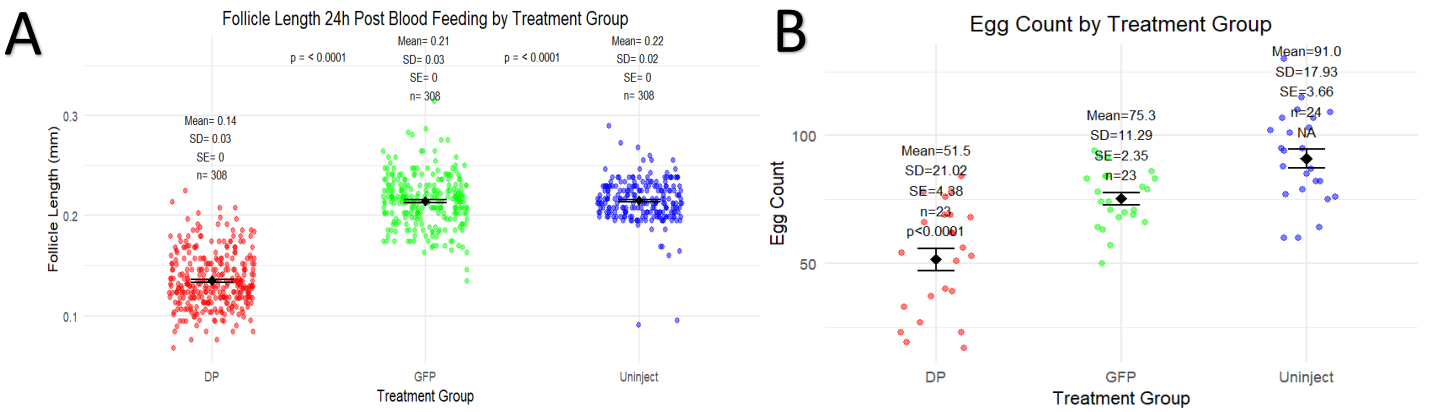

Figure 18. RNAi-mediated DP downregulation on A. aegypti reproduction and gene expression. (A) *Scatter plot comparing follicle lengths 24h post blood meal across different treatment groups, with red representing the DP group, green the GFP group, and blue the uninjected group.* ***(B)*** *The egg count per female is indicated by the same color scheme as in A, with statistical significance denoted where applicable.*

aegypti Aag2 cells. For the Co-IP experiment, cell lysates were incubated with beads coated with either rabbit IgG (negative control, lanes 1 and 2) or myc-specific IgG (lanes 3-6) (**Fig 20**). The beads, coated with Protein A/G, bind to the Fc region of antibodies. When MYC IgG is added, the beads specifically bind to the MYC IgG antibody,

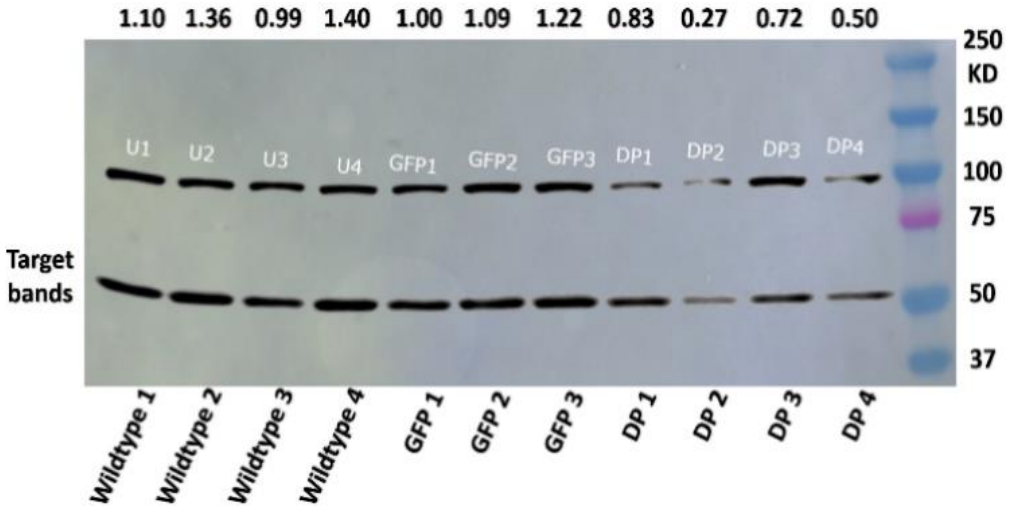

Figure 19. Western Blotting to Measure Efficacy of Injected dsRNA DP-1*. (A) Post-injection, mosquito abdomens are cut and ground with RIPA buffer and inhibitors. Denatured proteins are separated by SDS-PAGE, transferred to a membrane, and probed with specific antibodies. The membrane is then scanned to assess the protein levels, determining the efficacy of the dsRNA injection.* ***(B)*** *Western blot analysis with each lane loaded with proteins pooled from five mosquitoes, assessing DP protein levels. The gel includes lanes for wildtype (U1-U4), GFP control (GFP1-GFP3), and DP RNAi-treated (DP1-DP4) groups, alongside a molecular weight marker (right). The numbers at the top of the figure represent the relative band intensity, normalized to the GFP1 control.*

allowing the capture of myc-Kr-h1 and associated proteins (KAPs) in the lysate. Immunoprecipitated complexes were then analyzed by Western blotting.

The Co-IP results showed no binding activity in the rabbit IgG control (lanes 1 and 2), as evidenced by the absence of bands in the IP group, confirming the absence of non-specific interactions of DP-Kr-h1 complexes with the beads. In contrast, lanes 3 and 4, which included myc IgG, displayed distinct bands, indicating the successful co-elution of DP-Kr-h1 complexes. This interaction was validated by the presence of bands in both anti-myc and anti-DP blots in the IP group, demonstrating effective capture of the complexes. Lanes 5 and 6, which lacked myc-Kr-h1, did not show any band formation, confirming that DP-HA could not be co-immunoprecipitated without myc-Kr-h1, despite the presence of MYC IgG. The observed bands, approximately 50 kDa, correspond to the expected size of DP, affirming the specific interaction between DP and Kr-h1 in Aag2 cells.

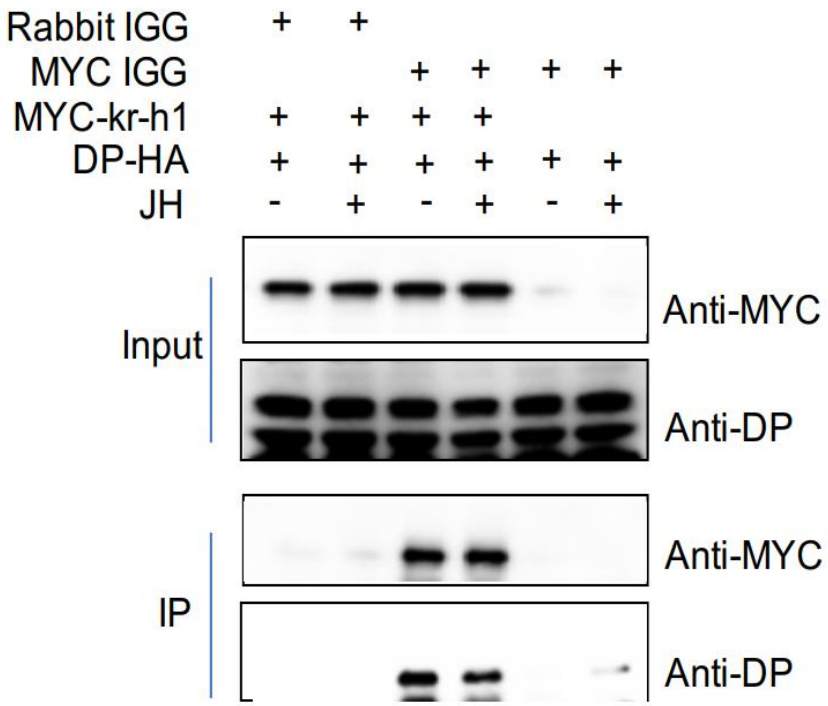

Figure 20. Co-immunoprecipitation analysis of MYC-kr-h1 and DP-HA interactions in the presence of juvenile hormone (JH). *Protein extracts from cells co-expressing MYC-tagged kr-h1 and HA-tagged DP were subjected to immunoprecipitation (IP) with MYC antibody or control Rabbit IgG, followed by Western blotting. The 'Input' lanes confirm the expression of MYC-kr-h1 and DP-HA proteins in the cell lysates. The 'IP' lanes reveal the presence of DP-HA when precipitated with MYC IGG antibody, indicating an interaction between kr-h1 and DP, modulated by JH treatment.*

The band intensity in lanes 3 and 4 from the IP group revealed that JH did not visibly affect the specific binding between Kr-h1 and DP-1. Similar band patterns were observed regardless of JH treatment, suggesting that JH does not alter the interaction between these proteins under the given experimental conditions.

Chapter 3: Discussion

3.1 The mRNA Transcription Profiles of KAPs

The preliminary analysis focused on the mRNA expression profiles of Kr-h1 associated proteins (KAPs)—ZnF_AD, SET, and DP-1—in the fat body of wildtype female *A. aegypti* at various stages during previtellogenic stage (post-eclosion) and vitellogenic stage (post-blood feeding). The results indicated that the relative transcript levels of DP-1 were significantly higher compared to ZnF_AD and SET at 12h PB. Specifically, DP-1 expression showed a marked increase at this time point, suggesting its potential involvement in early vitellogenesis.

The crucial role of Kr-h1 in the reproductive processes of *A. aegypti*, particularly in regulating genes involved in vitellogenesis under the influence of juvenile hormone (JH) and 20-hydroxyecdysone (20E), has been confirmed in many studies[44-47]. Kr-h1 is a transcription factor induced by JH and plays a critical role in regulating gene expression during insect development and reproduction. Upon JH binding to its receptor, Methoprene-tolerant (Met), the heterodimer Met-Taiman (Tai) complex forms and binds to JH response elements (JHREs) on the promoters of target gene, leading to the activation of Kr-h1 transcription. Kr-h1 can act as both a repressor and an activator, depending on the promoter sequences. Kr-h1 can repress the expression of genes involved in metamorphosis by inhibiting ecdysone-induced TFs while promoting the expression of genes necessary for vitellogenesis and other reproductive processes during the adult stage. The specific expression patterns and potential regulatory roles of its KAPs, however, have not been extensively studied. Our findings reveal that DP-1 may have a critical role during early vitellogenesis, aligning with the timing of peak JH levels and subsequent Kr-h1 activity. This suggests that DP-1 could be a key player in the regulatory network governed by Kr-h1 during mosquito reproduction.

The pronounced expression of DP-1 spikes at 12 PBM, likely due to activation by raw materials from the digested blood. This activation involves interactions with key transcription factors such as E2F and plays a crucial role in cell cycle regulation, essential for vitellogenesis and egg maturation during the reproductive phase. In contrast, ZnF_AD and SET may have less critical roles during these stages or may be involved in other physiological processes not covered by this study.

This distinctive expression pattern underscores DP-1's crucial role in *A. aegypti* vitellogenic physiology, suggesting its potential as a pivotal modulator within the JH signaling pathway. This aligns with its regulatory influence alongside Kr-h1 on downstream genes that are critical for egg development. By

delineating the specific functions of DP-1, our study enhances understanding of mosquito fecundity mechanisms and identifies novel targets for mosquito population control strategies. Thus, it contributes to a deeper grasp of the intricate networks governed by JH and Kr-h1, emphasizing the significance of DP-1 in these regulatory processes.

3.2 RNA Interference (RNAi) Effects on KAPs Expression and Reproduction

The second objective involved employing RNA interference (RNAi) to repress the expression of target potential KAPs (ZnF_AD, SET, and DP-1) and assess the effects on follicle length and egg production in *A. aegypti*. The results demonstrated that while the mRNA levels of all three KAPs were significantly downregulated by their respective custom dsRNA primers, only the group injected with dsRNA targeting DP-1 showed a marked reduction in follicle length compared to the GFP control and wildtype groups, particularly at 24 hours post-blood feeding (PB). Further injections confirmed the consistency of this phenotype, with DP-1 knockdown mosquitoes consistently displaying smaller follicles. Furthermore, the quantity of eggs laid by mosquitoes with DP-1 knockdown suggests a correlation between DP-1 levels and fecundity (**Fig 16B**). The WB confirmed these findings at the protein level, showing weaker signals for DP-1 protein in the dsRNA DP-1 injected group, with 2 bands displaying particularly low levels of DP-1 protein (**Fig 19B**). Our findings align with studies showing that JH and Kr-h1 are vital for follicle development and egg production, but they add a new dimension by implicating DP-1 as a crucial modulator within this pathway. The downregulation of DP-1 not only disrupts Kr-h1-associated transcriptional regulation but also directly impacts follicle development and fecundity, indicating a more complex Kr-h1 interaction network than previously understood.

The significant reduction in follicle length and egg production in the DP-1 knockdown group likely reflects DP-1's role in essential reproductive processes. DP-1 might interact with critical transcription factors or signaling molecules involved in cell cycle regulation and growth, which are necessary for vitellogenesis and egg maturation. The lack of similar phenotypic changes in the ZnF_AD and SET knockdown groups suggests functional redundancy or that these proteins have roles outside the specific reproductive stages analyzed. Some mosquitoes injected with dsRNA did not exhibit reduced transcript levels compared to the GFP control, as evidenced by the enlarged error bars (**Fig 15**). The injected dsRNA might did not effectively bind to the Dicer enzyme, which is crucial for RNA-induced silencing complex (RISC) formation. Without proper binding, the dsRNA would fail to guide the RISC to the target mRNA, leading to no reduction in transcript levels. Alternatively, the dsRNA might have been degraded by endogenous

RNases before it could reach its target, or it may not have been efficiently absorbed by some of the cells exclude from fat body.

The variation in protein intensity observed in the WB, despite each tube containing five dsRNA DP-1 injected mosquitoes' abdomens, could be due to post-transcriptional and post-translational modifications that affect protein stability and degradation rates. These modifications might vary among individual mosquitoes and affect the amount of detectable protein, even when starting with equal quantities. Another consideration is the potential impact of biological variability in the expression and regulation of other interacting proteins or co-factors that influence the stability and detection of DP-1.

In addition, despite ZnF_AD and SET didn't show any obvious phenotypic change related to follicle length, they would play critical roles during other developmental stages, such as larvae or pupae, rather than adult reproduction. These proteins might be involved in processes that are not active or necessary during the reproductive stage analyzed in this study. Alternatively, ZnF_AD and SET might have redundant functions with other proteins that compensate for their knockdown, masking any potential phenotypic effects.

The results from RNAi experiments underscore DP-1's critical role in *A. aegypti* reproduction, further positioning it as a key regulator within the broader network of vitellogenic processes. The obvious effect of DP-1 knockdown on follicle development and egg production suggests that DP-1 is integral to the proper execution of these processes.

3.3 Co-Immunoprecipitation (Co-IP) Analysis of Kr-h1 and AaDP-1 Interactions

The Co-IP experiment provided insight into the interaction between Kr-h1 and DP proteins, highlighting both specific and potential JH-modulated interactions. The absence of bands in the rabbit IgG control confirms the specificity of the immunoprecipitation process, indicating no non-specific binding of DP-Kr-h1 complexes. The presence of clear bands in the lanes with myc-specific IgG demonstrates a successful co-elution of DP-Kr-h1 complexes, validating the interaction between these proteins.

A notable observation was the slight band detected in lane 6 with anti-DP in the presence of JH, despite the absence of myc-Kr-h1. This suggests that JH may facilitate weak or transient interactions involving DP-HA. One possible explanation is that JH alters the protein environment, promoting non-specific binding or stabilizing weak interactions between DP-HA and other proteins or components within the lysate. This could result in DP-HA being indirectly captured by the beads via these weak associations.

The analysis indicated that JH did not significantly impact the specific interaction between Kr-h1 and DP-1, as evidenced by the consistent band patterns in lanes 3 and 4, regardless of JH presence. This suggests that the primary interaction between Kr-h1 and DP is robust and not influenced by JH under the experimental conditions used. However, the weak interaction observed in lane 6 warrants further investigation to elucidate the potential roles of JH in modulating protein complexes involving DP-HA. Understanding the specific functions and interactions of DP-1 could provide deeper insights into the molecular mechanisms of JH action in *A. aegypti* vitellogenesis and reproduction. These findings contribute to a more comprehensive understanding of the molecular mechanisms driving mosquito fecundity, highlighting the potential for innovative vector control strategies. Future studies should focus on exploring the nature of the JH-induced interactions, potentially through more refined protein interaction assays or using different experimental conditions to determine the biological significance of these observations.

3.4 Future Directions for Chromatin Binding Gene Regulation and AaDP-1 and Kr-h1 Mechanisms Conservation

To further elucidate the molecular mechanisms underlying the interaction between DP-1 and Kr-h1, future studies will employ CUT&RUN (Cleavage Under Targets and Release Using Nuclease) analysis (**Fig 20**). This technique will help in mapping the chromatin binding profiles of both DP-1 and Kr-h1 in the fat body tissue of *A. aegypti*. Several critical questions need to be addressed. Firstly, it is essential to determine whether there is an overlap in the target promoters bound by DP-1 and

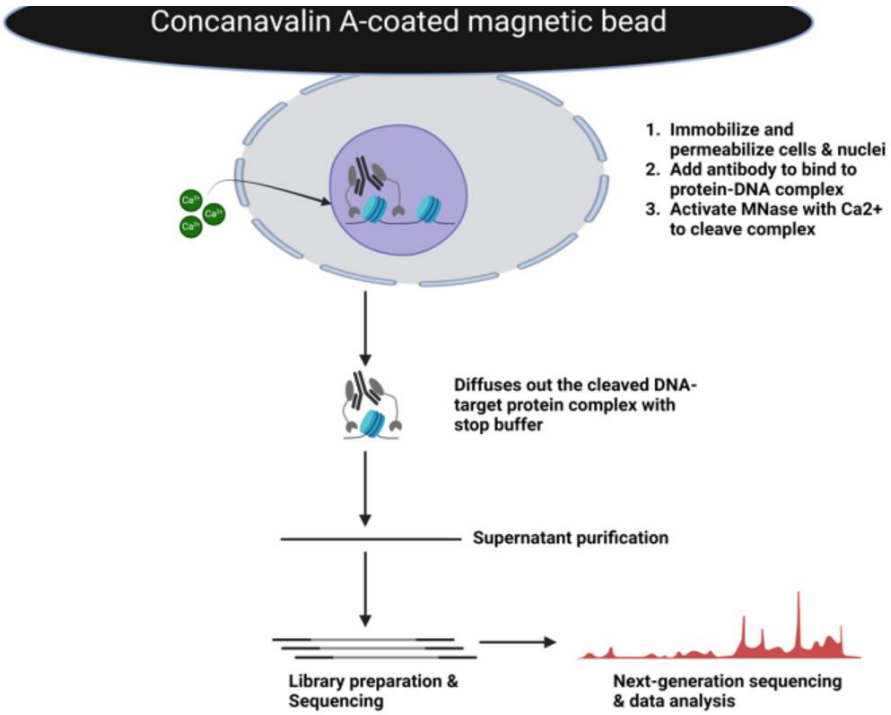

Figure 20: procedures of CUT&RUN. *Cells are immobilized on concanavalin A-coated magnetic beads. An antibody specific to the target complex is added along with MNase, which is activated by Ca2+ to cleave the DNA at target sites. The cleaved DNA-protein complexes are then released and purified from the supernatant. The purified DNA is prepared for sequencing and analyzed using next-generation sequencing to identify binding sites, generating high-resolution maps of protein-DNA interactions.*

Kr-h1. This will involve identifying common binding sites and evaluating the extent of co-localization on chromatin. Additionally, it will be assessed whether the absence of one protein affects the binding efficiency or pattern of the other on chromatin sites by knocking down the expression of DP-1 or Kr-h1 respectively and keep verified with RNAi and WB. This will help in understanding the interdependency of their binding.

Furthermore, it will be investigated whether knocking down DP-1 influences the expression of genes that are bound by both DP-1 and Kr-h1. This analysis will provide insights into the regulatory hierarchy and potential compensatory mechanisms within the JH signaling pathway. Moreover, the impact of DP-1 knockdown on histone modifications at promoters bound by both DP-1 and Kr-h1 will be examined. This will involve profiling histone marks associated with active or repressive chromatin states to understand how DP-1 modulates chromatin structure and gene expression.

In addition to these molecular studies, the conservation of the DP-1 and Kr-h1 interaction mechanism will be explored in other mosquito species and fruit flies. Specifically, it will be investigated whether the interactions between DP-1 and Kr-h1 are conserved in other mosquito species, such as *Aedes albopictus*, *Anopheles gambiae*, and in model organisms like *Drosophila melanogaster*. By examining these interactions in different species, the aim is to determine the evolutionary conservation and functional significance of these regulatory mechanisms.

Moreover, the necessity of these interactions for JH responses in these species will be assessed with Co-IP. This will involve evaluating the functional roles of DP-1 and Kr-h1 in JH signaling pathways across different insect species, providing a comparative analysis of their roles in insect physiology.

These future studies will provide a deeper understanding of the regulatory networks involving DP-1 and Kr-h1 and their broader implications in insect physiology. By addressing these questions, potential targets for innovative vector control strategies that disrupt mosquito reproduction without affecting non-target organisms can be uncovered. Through this comprehensive approach, contributing to the development of more effective and ecologically sound methods for global vector-borne diseases control can be more feasible.

References

1. Leta, S., Beyene, T. J., De Clercq, E. M., Amenu, K., Kraemer, M. U., & Revie, C. W. (2018). Global risk mapping for major diseases transmitted by *Aedes aegypti* and *Aedes albopictus*. International journal of infectious diseases, 67, 25-35.
2. Moore, C. A., Staples, J. E., Dobyns, W. B., Pessoa, A., Ventura, C. V., Da Fonseca, E. B., ... & Rasmussen, S. A. (2017). Characterizing the pattern of anomalies in congenital Zika syndrome for pediatric clinicians. JAMA pediatrics, 171(3), 288-295.
3. Beckham, J. D., Pastula, D. M., Massey, A., & Tyler, K. L. (2016). Zika virus as an emerging global pathogen: neurological complications of Zika virus. JAMA neurology, 73(7), 875-879.
4. Grabenstein, J. D., & Tomar, A. S. (2023). Global geotemporal distribution of chikungunya disease, 2011–2022. Travel Medicine and Infectious Disease, 102603.
5. Lataillade, L. D. G. D., Vazeille, M., Obadia, T., Madec, Y., Mousson, L., Kamgang, B., ... & Yen, P. S. (2020). Risk of yellow fever virus transmission in the Asia-Pacific region. Nature communications, 11(1), 5801.
6. Kimble, J. B., Noronha, L., Trujillo, J. D., Mitzel, D., Richt, J. A., & Wilson, W. C. (2024). Rift Valley Fever. Veterinary Clinics: Food Animal Practice.
7. Powell, J. R. (2018). Mosquito-borne human viral diseases: why Aedes aegypti?. The American journal of tropical medicine and hygiene, 98(6), 1563.
8. Kraemer, M. U., Reiner Jr, R. C., Brady, O. J., Messina, J. P., Gilbert, M., Pigott, D. M., ... & Golding, N. (2019). Past and future spread of the arbovirus vectors Aedes aegypti and Aedes albopictus. Nature microbiology, 4(5), 854-863.
9. Smith, L. B., Kasai, S., & Scott, J. G. (2016). Pyrethroid resistance in *Aedes aegypti* and *Aedes albopictus*: Important mosquito vectors of human diseases. Pesticide biochemistry and physiology, 133, 1-12.
10. Bhatt, S., et al. (2013). The global distribution and burden of dengue. Nature, 496(7446), 504–507.
11. Weaver, S. C., & Reisen, W. K. (2010). Present and future arboviral threats. Antiviral Research, 85(2), 328–345.
12. Benelli, G., & Mehlhorn, H. (2016). Declining malaria, rising of dengue and Zika virus: insights for mosquito vector control. Parasitology Research, 115(5), 1747–1754.
13. Invest, J. F., & Lucas, J. R. (2008). Pyriproxyfen as a mosquito larvicide.

14. Egid, B. R., Coulibaly, M., Dadzie, S. K., Kamgang, B., McCall, P. J., Sedda, L., ... & Wilson, A. L. (2022). Review of the ecology and behaviour of *Aedes aegypti* and *Aedes albopictus* in Western Africa and implications for vector control. Current research in parasitology & vector-borne diseases, 2, 100074.
15. Goodman, W. G., & Granger, N. A. (2005). The Juvenile Hormones. In Comprehensive Molecular Insect Science (Elsevier), Vol. 3, pp. 319–408.
16. Riddiford, L. M. (2012). How does juvenile hormone control insect metamorphosis and reproduction? General and Comparative Endocrinology, 179(3), 477–484.
17. Hemingway, J., et al. (2016). Averting a malaria disaster: will insecticide resistance derail malaria control? Lancet, 387(10029), 1785–1788.
18. Liu, N., et al. (2017). Insecticide resistance in mosquito vectors. Nature Reviews Microbiology, 15(5), 384–396.
19. Raikhel, A. S., et al. (2002). Molecular biology of mosquito vitellogenesis: from basic studies to genetic engineering of antipathogen immunity. Insect Biochemistry and Molecular Biology, 32(10), 1275–1286.
20. Noriega, F. G. (2014). Nutritional regulation of JH synthesis: a mechanism to control reproductive maturation in mosquitoes? Insect Biochemistry and Molecular Biology, 56, 34–40.
21. Zhu, J., and F. G. Noriega. "The role of juvenile hormone in mosquito development and reproduction." Advances in insect physiology. Vol. 51. Academic Press, 2016. 93-113.
22. Liu P, Peng HJ, Zhu J. Juvenile hormone-activated phospholipase C pathway enhances transcriptional activation by the methoprene-tolerant protein. Proceedings of the National Academy of Sciences. 2015 Apr 14;112(15):E1871-9.
23. Zhu, J. (2022). Non-genomic action of juvenile hormone modulates the synthesis of 20-hydroxyecdysone in Drosophila. Science bulletin, 67(2), 117.
24. He, Q., & Zhang, Y. (2022). Kr-h1, a cornerstone gene in insect life history. Frontiers in Physiology, 13, 905441.
25. Ashok M, Turner C, Wilson TG (1998) Insect juvenile hormone resistance gene homology with the bHLH-PAS family of transcriptional regulators. Proc Natl Acad Sci USA 95:2761–2766.
26. Charles JP, et al. (2011) Ligand-binding properties of a juvenile hormone receptor, methoprene-tolerant. Proc Natl Acad Sci USA 108:21128–21133.
27. Jindra M, Uhlirova M, Charles JP, Smykal V, Hill RJ (2015) Genetic evidence for function of the bHLH-PAS protein Gce/Met as a juvenile hormone receptor. PLoS Genet 11:e1005394.

28. Rogers, Kara. "avian malaria". Encyclopedia Britannica, 18 Mar. 2019, https://www.britannica.com/science/avian-malaria. Accessed 1 April 2024.
29. Du, Y., Nomura, Y., Zhorov, B. S., & Dong, K. (2016). Sodium channel mutations and pyrethroid resistance in Aedes aegypti. *Insects*, *7*(4), 60.
30. Gao, Y., Liu, S., Jia, Q., Wu, L., Yuan, D., Li, E. Y., ... & Li, S. (2022). Juvenile hormone membrane signaling phosphorylates USP and thus potentiates 20-hydroxyecdysone action in Drosophila. Science Bulletin, 67(2), 186-197.
31. Hustedt, J. C., Boyce, R., Bradley, J., Hii, J., & Alexander, N. (2020). Use of pyriproxyfen in control of *Aedes* mosquitoes: A systematic review. PLoS neglected tropical diseases, 14(6), e0008205.
32. Yadav, K., Dhiman, S., Acharya, B. N., Ghorpade, R. R., & Sukumaran, D. (2019). Pyriproxyfen treated surface exposure exhibits reproductive disruption in dengue vector Aedes aegypti. PLoS Neglected Tropical Diseases, 13(11), e0007842.
33. Evaluating the sterilizing effect of pyriproxyfen-treated mosquito nets against Anopheles gambiae at different blood-feeding intervals
34. Jindra, M., & Bittova, L. (2020). The juvenile hormone receptor as a target of juvenoid “insect growth regulators”. Archives of insect biochemistry and physiology, 103(3), e21615.
35. Gospocic, J., Glastad, K. M., Sheng, L., Shields, E. J., Berger, S. L., & Bonasio, R. (2021). Kr-h1 maintains distinct caste-specific neurotranscriptomes in response to socially regulated hormones. Cell, 184(23), 5807-5823.
36. Minakuchi, C., Zhou, X., & Riddiford, L. M. (2008). Krüppel homolog 1 (Kr-h1) mediates juvenile hormone action during metamorphosis of Drosophila melanogaster. Mechanisms of development, 125(1-2), 91-105.
37. Ling, L., & Raikhel, A. S. (2021). Cross-talk of insulin-like peptides, juvenile hormone, and 20-hydroxyecdysone in regulation of metabolism in the mosquito Aedes aegypti. Proceedings of the National Academy of Sciences, 118(6), e2023470118.
38. Gulia-Nuss, M., Robertson, A. E., Brown, M. R., & Strand, M. R. (2011). Insulin-like peptides and the target of rapamycin pathway coordinately regulate blood digestion and egg maturation in the mosquito Aedes aegypti. PloS one, 6(5), e20401.
39. Kayukawa, T., Minakuchi, C., Namiki, T., Togawa, T., Yoshiyama, M., Kamimura, M., ... & Shinoda, T. (2012). Transcriptional regulation of juvenile hormone-mediated induction of Krüppel homolog 1, a

repressor of insect metamorphosis. Proceedings of the National Academy of Sciences, 109(29), 11729-11734.

40. Kayukawa, T., Nagamine, K., Ito, Y., Nishita, Y., Ishikawa, Y., & Shinoda, T. (2016). Krüppel homolog 1 inhibits insect metamorphosis via direct transcriptional repression of Broad-Complex, a pupal specifier gene. Journal of Biological Chemistry, 291(4), 1751-1762.
41. Li, K. L., Yuan, S. Y., Nanda, S., Fu, Q., & Wan, P. J. (2018). The roles of E93 and Kr-h1 in metamorphosis of Nilaparvata lugens. Frontiers in Physiology, 9, 410502.
42. Kayukawa, T., Nagamine, K., Ito, Y., Nishita, Y., Ishikawa, Y., & Shinoda, T. (2016). Krüppel homolog 1 inhibits insect metamorphosis via direct transcriptional repression of Broad-Complex, a pupal specifier gene. Journal of Biological Chemistry, 291(4), 1751-1762.
43. Wu, Z., Yang, L., Li, H., & Zhou, S. (2021). Krüppel-homolog 1 exerts anti-metamorphic and vitellogenic functions in insects via phosphorylation-mediated recruitment of specific cofactors. BMC biology, 19, 1-14.
44. Ojani, R., Fu, X., Ahmed, T., Liu, P., & Zhu, J. (2018). Krüppel homologue 1 acts as a repressor and an activator in the transcriptional response to juvenile hormone in adult mosquitoes. Insect molecular biology, 27(2), 268-278.
45. Ojani, R., Liu, P., Fu, X., & Zhu, J. (2016). Protein kinase C modulates transcriptional activation by the juvenile hormone receptor methoprene-tolerant. Insect biochemistry and molecular biology, 70, 44-52.
46. Wu, Z., Yang, L., He, Q., & Zhou, S. (2021). Regulatory mechanisms of vitellogenesis in insects. Frontiers in Cell and Developmental Biology, 8, 593613.
47. Sheng, Z., Xu, J., Bai, H., Zhu, F., & Palli, S. R. (2011). Juvenile hormone regulates vitellogenin gene expression through insulin-like peptide signaling pathway in the red flour beetle, Tribolium castaneum. Journal of Biological Chemistry, 286(49), 41924-41936.
48. Brayer, K. J., & Segal, D. J. (2008). Keep your fingers off my DNA: protein–protein interactions mediated by C2H2 zinc finger domains. Cell biochemistry and biophysics, 50, 111-131.